

**OPTIMIZATION OF A FLUID BED DRYER BY THE IMPLEMENTION OF A  
MODEL PREDICTIVE CONTROLLER**

By

Joshel Omar Rivera Pacheco

A thesis submitted in partial fulfillment of the requirements for the degree of

MASTER IN SCIENCE  
in  
CHEMICAL ENGINEERING

UNIVERSITY OF PUERTO RICO  
MAYAGÜEZ CAMPUS

May, 2006

Approved by:

\_\_\_\_\_  
Jeanette Santos Cordero, Ph.D.  
Member, Graduate Committee

\_\_\_\_\_  
Date

\_\_\_\_\_  
Moses Bogeres, Ph.D.  
Member, Graduate Committee

\_\_\_\_\_  
Date

\_\_\_\_\_  
Carlos Velázquez Figueroa, Ph.D.  
President, Graduate Committee

\_\_\_\_\_  
Date

\_\_\_\_\_  
Felix Román, Ph.D.  
Representative of Graduate Studies

\_\_\_\_\_  
Date

\_\_\_\_\_  
Nelson Cardona Martínez, Ph.D.  
Chairperson of the Department

\_\_\_\_\_  
Date

## Abstract

Optimization of the drying operation requires a model containing the operating variables for fluid bed dryers (FBD). Modeling of FBD is still uncertain since the drying process is unpredictable and relies on empirical parameters. The objective was to develop a first principle model that would describe the moisture content of a pharmaceutical powder as function of operating variables and use it for optimization purposes. Granulations consisting of lactose monohydrate, pregelatinized starch, and distilled water were dried in a FBD to generate the data to develop the models. Basic energy and material balances led to the description of the drying curve and it was used to determine the parameters necessary to design a customized Model Predictive Controller (MPC).

The simulation shows that by implementing an MPC the desired set point is achieved in half the time and consumes less energy as compared to working at the FBD's maximum settings. Compared to traditional MPC, this customized controller provided a more logical response of the drying process since the traditional strategy is more accurate when it is applied to stable processes. Compared to a Proportional-Integral-Derivative (PID) strategy, the MPC proved to be a better tool for optimizing the drying process.

## Resumen

La optimización del proceso de secado requiere un modelo que contenga las variables de operación para una secadora de lecho fluidizado (FBD). El modelar el FBD sigue incierto ya que el proceso de secado es impredecible y depende de parámetros empíricos. El objetivo de este estudio ha sido el desarrollar un modelo fundamental que describa la humedad de un polvo farmacéutico y utilizarlo para propósitos de optimización. Las granulaciones, que consistieron de lactosa monohidratada y almidón pregelatinizado combinado con agua destilada, fueron secadas en un FBD para generar los datos para desarrollar el modelo. Utilizando balances básicos de energía y materiales se obtuvo la descripción de la curva de secado y se utilizó para determinar los parámetros necesarios para diseñar el controlador de modelo predictivo (MPC) modificado.

Las simulaciones demostraron que por la implementación del MPC el valor deseado se obtuvo en la mitad del tiempo y consumió menos energía comparado a trabajar la secadora en su máxima capacidad constantemente. Comparado con la estrategia tradicional de MPC, el controlador modificado proveyó con una respuesta más lógica del proceso de secado ya que la estrategia tradicional es más precisa cuando es aplicado a un proceso estable. Comparado con una estrategia de control Proporcional-Integral-Derivativa (PID), el MPC demostró ser una mejor herramienta para optimizar el proceso de secado.

## Table of Content

<b>Chapter 1: Introduction</b>	<b>1</b>
1.1 Justification	1
1.2 Objectives	2
<b>Chapter 2: Background and Literature Review</b>	<b>3</b>
2.1 Case Studies	3
2.2 Model Predictive Control Strategy	4
2.3 Drying Curve Model	7
<b>Chapter 3: Materials and Methodology</b>	<b>15</b>
3.1 Materials for drying curves experiments	15
3.2 Equipment for drying curves experiments	15
3.3 Methodology for drying curves experiments	17
<b>3.3.1 Powder weighing</b>	<b>17</b>
<b>3.3.2 Wet granulation preparation</b>	<b>17</b>
3.4 Fluid Bed Drying	18
3.5 LOD Moisture Analyzer	19
<b>Chapter 4: First Principle Model</b>	<b>20</b>
4.1 Development of the Drying Curve Model	20
4.2 First Principle Model Results	24
<b>Chapter 5: Development of the Model Predictive Controller</b>	<b>28</b>
5.1 MPC Design	28
5.2 Simulation Result	30
5.3 Stability Test for the MPC	33
<b>Chapter 6: Other Approaches to MPC Design</b>	<b>36</b>
6.1 Step-response MPC	36
6.2 State-space MPC	40
<b>Chapter 7: Development of a PID Controller</b>	<b>46</b>
7.1 PID Design	46
7.2 Simulation Results	48
<b>Chapter 8: Conclusions and Recommendations</b>	<b>52</b>
8.1 Conclusions	52
8.2 Recommendations	54

<b>References</b>	<b>55</b>
<b>Appendix A. Parameter Definition for the First Principle Model</b>	<b>57</b>
<b>Appendix B. Drying Curves at Different Operational Conditions</b>	<b>60</b>
<b>Appendix C. Model Predictive Control Algorithms</b>	<b>65</b>

## List of Tables

Table 3.1: List of ingredients for pharmaceutical granulation	15
Table 3.2: Operating conditions used at the FBD	19
Table 4.1: Values of $K_q$ at different operational conditions	25
Table 4.2: Values of $K_t$ at different operational conditions	25
Table 4.3: Values of $\tau$ at different operational conditions	26
Table 4.4: $R^2$ and standard deviation of the FPM at different operating conditions	26
Table 5.1: Relationships between the process model and MPC parameters. $\gamma_r^2$ is the diagonal element of $Q$ and $\lambda_s^2$ is the diagonal element of $R$ .	29
Table 5.2: Initial values of MPC parameters	30
Table 5.3: Final values of the MPC parameters	30
Table 5.4: Comparison between operational monitoring done by the MPC and an operator for airflow changes	32
Table 5.5: Comparison between operational monitoring done by the MPC and an operator for temperature changes	32
Table 7.1: PI Control parameters	47

## List of Figures

Figure 2.1: General block diagram of a Model Predictive Control Algorithm (Edgar, Mellichamp & Seaborg, 2004)	7
Figure 2.2: Model representation of drying process (Arocho 2004)	8
Figure 2.3: Graphical representation of drying process (Arocho 2004)	8
Figure 2.4: Hybrid model prediction of residual moisture content curves (Montenegro 2000)	9
Figure 3.1: Schematics diagram of Fluid Bed Dryer and control panel (Arocho 2004)	16
Figure 4.1: Prediction of drying curve using First Principle Model at airflow of 80 m <sup>3</sup> /hr and operating temperatures of 60 °C ( $\Delta T = 35^{\circ}\text{C}$ ) and 80 °C ( $\Delta T = 55^{\circ}\text{C}$ )	26
Figure 4.2: Comparison between the models using the Mass Transfer Coefficient and the FPM	27
Figure 5.1: Process response of the fluid bed dryer after implementing an MPC algorithm	31
Figure 5.2: Example of a root locus plot	34
Figure 5.3: Bode Diagram for the MPC design using the Drying Curve Model with constant parameters	35
Figure 6.1: Process response of the fluid bed dryer after implementing step-response MPC algorithm	39
Figure 6.2: Process response of the fluid bed dryer simulated by MPC toolbox in MATLAB®	43
Figure 6.3: Input changes calculated by the MPC toolbox in MATLAB® for the drying process in a fluid bed dryer	44

Figure 7.1: Block diagram representation of PID control model for a fluid bed dryer	48
Figure 7.2: Process response and input changes for the fluid bed dryer after PID implementation	49
Figure 7.3: Process response and input changes for the fluid bed dryer after physically bounded PID implementation	50



# Chapter 1: Introduction

## 1.1 Justification

The pharmaceutical process of creating a tablet or capsule consists of four steps: mixing, drying, milling, and tablet or capsule making. The drying process of grains or powder mixtures is one of the most important steps. If the mixture is too wet it can provide a medium to cultivate fungi, bacteria or other microorganisms. If the mixture is too dry the tablet cannot be made since the mixture would not bind together. For over 30 years the pharmaceutical industry has used many types of dryers. One of the most commonly used is fluid bed dryers for its capacity to dry large amounts of products and higher drying rates.

Up until now the modeling of the drying process has been limited, making the process less predictable. It has been established that the drying process consists of four stages. Yet the determination of the drying curve function is not fully known. Many investigators have determined empirical equations that describe the drying curve using as a basis fundamental equations such as the mass and energy balances around the drying process. The problem lies in the implementation of these equations at an industrial scale.

The determination of the pharmaceutical powder's humidity is at a level in which samples have to be taken and analysis done offline. At this level the most common operational procedure would be to maintain temperature and inlet flow constant. It has been proven that during the constant drying rate zone the phenomena occurring are heat and mass transfers and during the falling drying rate zone the phenomenon that dominates is diffusion. This means that unnecessary energy is being introduced into the drying process. By implementing a model predictive controller (MPC), it should be

expected to reduce the consumption of energy and improve performance of the fluid bed dryer. Also the MPC will be used to determine the optimal trajectory for the drying process, thereby reducing the drying time.

## 1.2 Objectives

The objectives of this research were:

- To develop a practical model to describe the drying curves of a pharmaceutical powder mixture in a fluid bed dryer.
- Compare the performance of different models in predicting moisture content.
- To develop a Model Predictive Controller (MPC) algorithm to lower the energy consumption of the fluid bed dryer and the drying time.
- Compare the fluid bed dryer performance under an MPC vs. PID control strategy.

## Chapter 2: Background and Literature Review

### 2.1 Case Studies

The first generations of MPC systems were developed in the 1970s by Shell Oil and ADERSA. The MPC control strategy began to be implemented during the 1980s at petrochemical plants (Cutler & Ramaker, 1980; Richalet *et al.*, 1978). Nowadays it is the control system mostly used in petrochemical plants over the world for multivariable control problems that include inequality constraints (Edgar, Mellichamp & Seaborg, 2004). Other industries have implemented MPC resulting in improvements in their processes. Baxter, by implementing an MPC system, was able to reduce batch distillation time by about 20 percent (Fiske & Ghosh, 2003). Kaneka Delaware Corporation (KDC), a producer of chemical and plastics, implemented an MPC system to their polyvinyl chloride (PVC) reactor to control the reactor's temperature, being able to reduce the temperature variability by 60 percent (Fiske & Ghosh, 2003). Before implementing MPC a highly complicated PID control system that used conservative temperature set point ramp rate was implemented at KDC. The problem with the reactor was that the control response was characterized by an open loop integrator with long delay and time constant.

A case study was conducted to implement an MPC in large scale operations (Morris, 1998). The study was focused on Anchor Products, Inc., a major manufacturer of Dairy Products in New Zealand. Anchor operates nine plants with combined capacity to convert 27.5 million L of milk per day into milk powders, milk proteins, cheese, and cream products all for exports. In 1994 they started up a new milk powder plant using a process control systems based on PLC (programmable logic controllers) and SCADA (supervisory control and data acquisition). But they also started to investigate how they

could optimize their evaporator and dryer by using MPC (model predictive control) software.

From the case studies of the Anchor plants (Morris, 1998), the primary control objectives for the evaporation stage were concentrate density and flow rate. The variables manipulated were fan speed, steam pressure and evaporator feed flow while the only disturbance variable was the condenser temperature. As a result of implementing a predictive controller it was possible to reduce variability in concentrate density up to 70%, the evaporators reached the desired target 95% faster for density control and they have minimized energy consumption and improved product quality. It was reported that the capacity of the evaporators were also increased up to 7 to 8%.

## 2.2 Model Predictive Control Strategy

The most common control algorithm is known as a PID (proportional-integral-derivative) controller. The PID algorithm is implemented in feedback control system in which the output of the process is compared to a set point (desired value) of the output. If the output is different from the set point, the controller adjusts the input to reach the set point. The problems that a PID controller have, in relation to the drying process, is that the controller does not take into consideration physical constraints of the process and that the implementation does not provide an opportunity to optimize a process in addition to reaching the desired set point.

The drying process, being a batch process, has as a physical constraint that the humidity of the powder cannot go below the equilibrium humidity. For the dryer to go beyond this equilibrium humidity it will be required to use more energy than the one used to reach it, which is not possible. If a PID controller is implemented the simulation of the

process might show an overshoot. This means that the controller is too aggressive that will make the process to pass the set point (which in this case is equilibrium humidity) and then would try to reach again the set point by changing the input. Besides the physical constraint, to return to the set point after the overshoot means that the dryer has to add moisture to the powder, which, obviously, is neither possible nor is it logical.

A predictive controller consists of three key elements: predictive model, optimization in a temporal window and feedback correction. The controller predicts process behavior and proactively optimizes control. Model predictive control (MPC) is a fairly general class of algorithms for feedback and feed forward control. Various MPC techniques have in common that a model of the process, subject for control, is used to predict the effects in process variables due to actual and future changes in manipulated outputs and feed-forward variables. The main objectives of an MPC, as proposed by Qin and Badgwell (Edgar, Mellichamp & Seaborg, 2004), are: 1) Prevent violations of input and output constraints. 2) Drive some output variables to their optimal set points while maintaining other outputs within specified ranges. 3) Prevent excessive movement of the input variables. 4) Control as many process variables as possible when a sensor or actuator is not available

The dynamic model [ $y(k) = G(q)u(k)$ ] that describes the real world process relates how manipulated outputs  $u(k)$ , from the operator or from a controller, affects the actual and future process variables  $y(k)$ . Further,  $G(q)$  is the discrete time transfer function for the process model. The process variables are measured signals that should follow desired set points  $r(k)$ .

The model predictive control objective could be defined as follows: Find a sequence of current and future changes in manipulated outputs  $\Delta u(k+i)$  that minimize a weighted sum of future squared control errors and a weighted sum of increments in the sequence of manipulated outputs  $\Delta u(k+i)$ , while limits for manipulated outputs and limits for predicted process variables are considered. This objective can be expressed mathematically: Find a sequence of increments for manipulated outputs  $\Delta u(k+i)$  over a control horizon of  $m$  samples:

$$J = \sum_{i=1}^p \|\Gamma e(k+i)\|_2^2 + \sum_{i=0}^{m-1} \|\Lambda \Delta u(k+i)\|_2^2 \quad \text{eq. 2.1}$$

subject to constraint :

$$\begin{aligned} y_{lo} &\leq y(k+i) \leq y_{hi} & \forall i \in [1, p] \\ u_{lo} &\leq u(k+i) \leq u_{hi} & \forall i \in [0, m-1] \\ \Delta u_{lo} &\leq \Delta u(k+i) \leq \Delta u_{hi} & \forall i \in [0, m-1] \end{aligned}$$

In this minimization the control errors  $e(k)=r(k)-y(k)$  (where  $r(k)$  is the humidity set point and  $y(k)$  the measured humidity) are considered over a prediction horizon of  $p$  future samples. The constraints for process variables  $y(k)$  are considered over a prediction horizon of  $p$  samples, and the constraints for manipulated outputs  $u(k)$ (air velocity and temperature) and their increments are considered over a control horizon of  $m$  future samples. In this procedure, the dynamic model is used for the prediction of future values for the process variables.

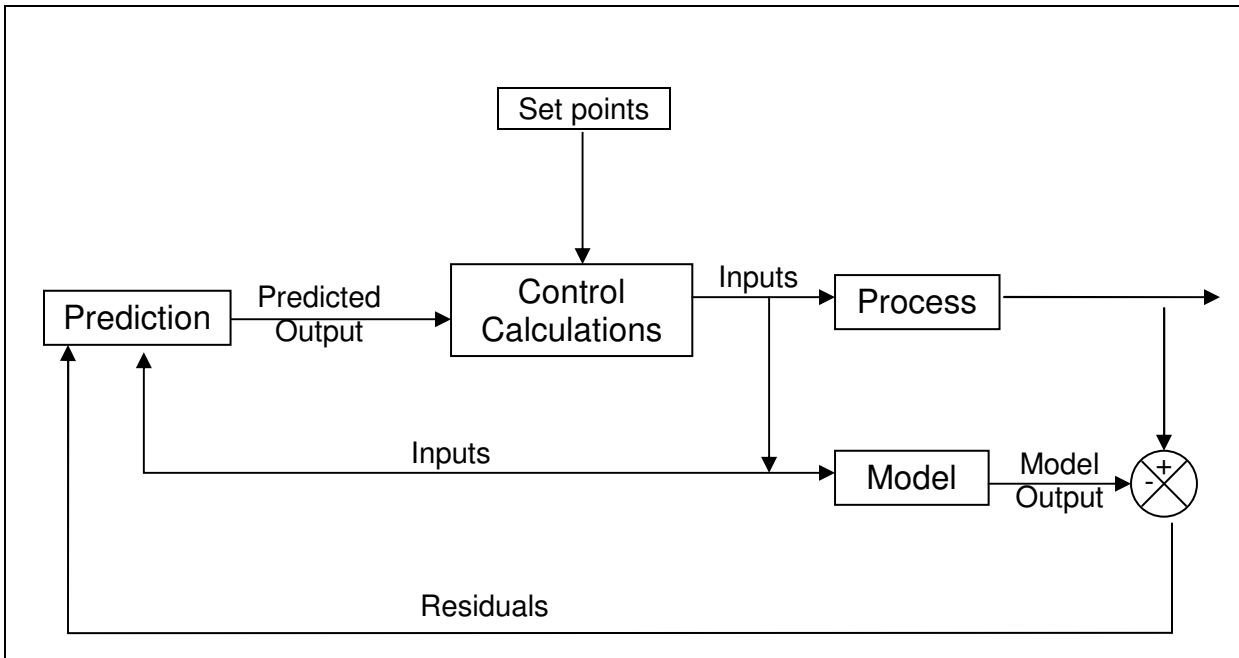


Figure 2.1: General block diagram of a Model Predictive Control algorithm (Edgar, Mellichamp & Seaborg, 2004)

### 2.3 Drying Curve Model

Drying is the removal of liquid by simultaneous heat and mass transfer. In FBD, the heat transfer rate to the water and then to the solid depends on the air temperature and flow, the exposed area (material's size), and pressure. Similarly, the mass transfer rate depends principally on the airflow and humidity, temperature, and exposed area.

As shown in Fig. 2.3, the drying curve consists of four stages: pre-heating, constant drying rate, falling drying rate, and dry surface diffusion. In each step, heat and mass transfer takes place, dominating the constant and falling drying rate regions. These phenomena contribute to the change in moisture content of the pharmaceutical powder. Many studies have been made to understand the behavior of the drying process. Alden *et al.* (1988) proposed the Temperature Difference Technique to model the moisture content:

$$w_p = f(\Delta T) \text{ eq. 2.2}$$

This model is based on adjustable parameters and a temperature drop. The adjustable parameters include the effect of air flow but it does not provide explicitly the drying time as an effect. Robinson (1992) presented the Temperature Drop model:

$$w_p = A (\Delta T)^b - C (\Delta t)^d \quad \text{eq. 2.3}$$

where  $A$ ,  $b$ ,  $C$ ,  $d$  again are adjustable parameters,  $\Delta T$  is the temperature drop in the direction of the flow and  $\Delta t$  is the drying time. Again this model is based on adjustable parameters where the effects of the air flow lay on them. Unlike Alden's model, Robinson's model does consider explicitly the effects of the drying time.

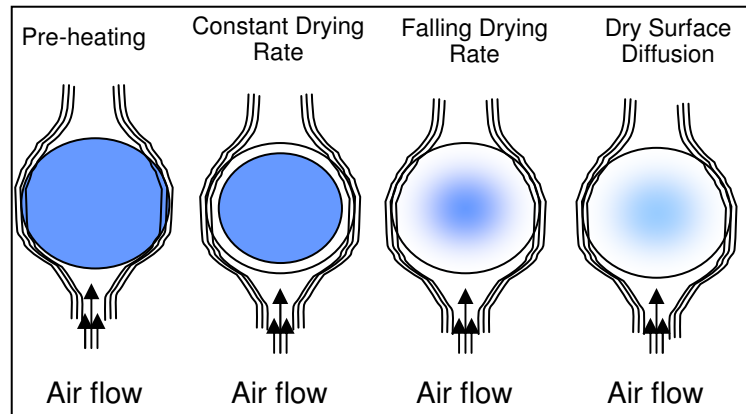


Figure 2.2: Model representation of drying process (Arocho 2004)

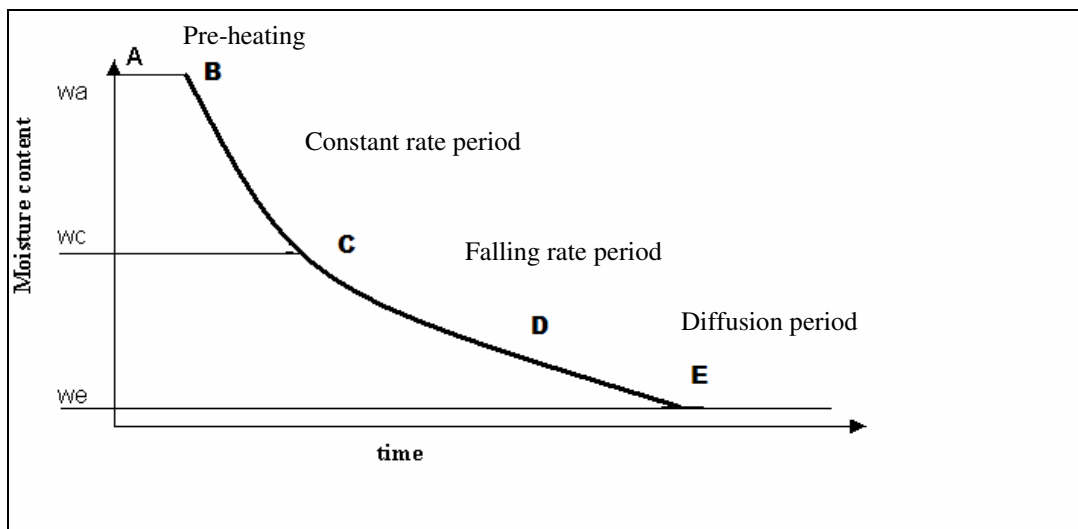


Figure 2.3: Graphical representation of drying process (Arocho 2004)



These proposed empirical models present two main limitations, namely each set of adjustable parameters is specific for a value of air flow and temperature and do not predict the entire drying curve as they do not consider different phenomena governing the process before and after the critical moisture content ( $w_c$ ). To overcome these limitations empirical equations have been developed by each individual researcher to describe each region of the drying curve.

Montenegro (2000) proposed a hybrid model using both Alden and Robinson's models for the drying curve. The constant rate region is controlled by external condition as long as the drying flux is linearly dependent on the mass transfer coefficient. This region is also dependent on initial humidity and drying rate. For a porous material the initial drying rate may remain constant over a wide range of moisture content, often ending this region at very low average moisture content ( $w_c$ ). Figure 2.4 depicts the prediction of the hybrid approach used by Montenegro using the fitted temperature drop model before the critical moisture content and the fitted temperature difference technique after that point.

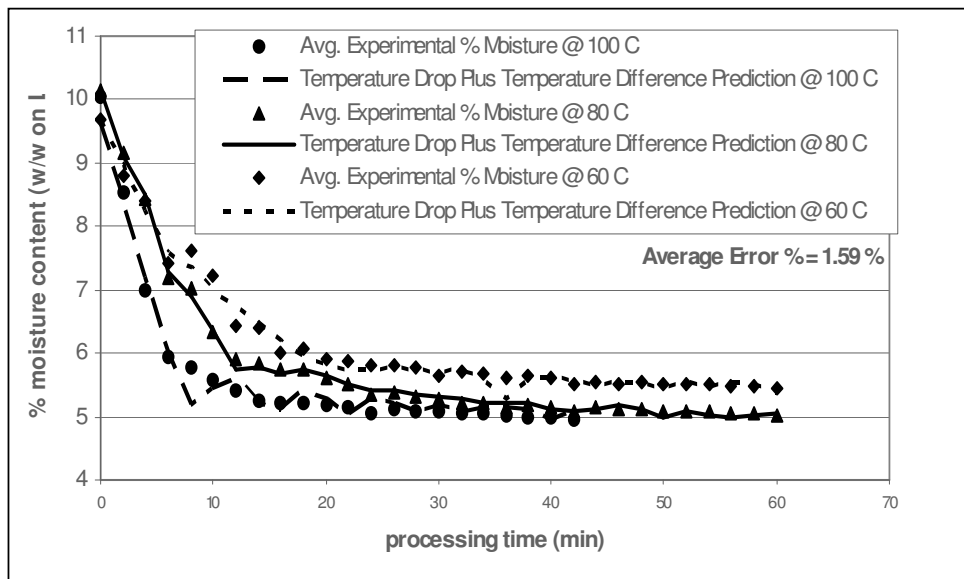


Figure 2.4: Hybrid model prediction of residual moisture content curves (Montenegro 2000)

Chandran, Subba and Varma (1990) developed a kinetic model to describe the fluid bed drying. For the constant rate period the moisture content is as follows:

$$w_p = w_{p_o} - kt \quad \text{eq. 2.4}$$

For the falling rate the model is:

$$w_p = w_p^+ + (w_{p_c} - w_p^+) \exp \left[ \frac{-k(t - t_c)}{(w_{p_c} - w_p^+)} \right] \quad \text{eq. 2.5}$$

Where  $w_{p_o}$ ,  $w_{p_c}$ , and  $w_p^+$  are the initial, critical and equilibrium moisture content respectively,  $R$  is the drying rate, expressed as weight of water evaporated per unit weight of dry material and unit time,  $t$  is the drying time, and  $t_c$  is the time where the moisture content is equal to the critical moisture content. The assumptions made to develop these kinetic models were:

1. The falling rate period is linear and is represented by a single line from the critical moisture content to the equilibrium moisture content.
2. The feed conditions of the heating medium remain unaltered during the drying process,
3. The contact area between the solids and the drying medium remains constant for the chosen gas-solid system and conditions.

Arocho (2004) developed a correlation that relates the mass transfer coefficient to the airflow and temperature, based on the works of Montenegro, Shinsky and Liptak. Having a constant drying rate means that the water flux towards the passing air is constant in this region. This water flux is dependent on the superficial area of exposure:

$$dm_w = -N_A dA \quad \text{eq. 2.6}$$

where

$$N_A = k_Y a (Y_{w,i} - Y_{w,b}) \quad \text{eq. 2.7}$$

$k_Y a$  = Mass transfer coefficient

$Y_{w,i}$  = Inter phase humidity

$Y_{w,b}$  = Bulk humidity of air

For the water-air system at steady state under adiabatic conditions, the energy supplied to evaporate the water flux is equal to the energy removed by the evaporated water:

$$h_g (T_g - T_w) = \lambda_w k_Y a (Y_{w,i} - Y_{w,b}) \quad \text{eq. 2.8}$$

where

$h_g$  = Heat transfer coefficient

$T_g$  = Bulk temperature of air

$T_w$  = Bulk temperature of water

$\lambda_w$  = Latent heat of water

Combining equations 2.6, 2.7, and 2.8 one obtains:

$$(w_2 - w_1) = \frac{A * \zeta}{m_{wp}} \ln \frac{(T_i - T_w)}{(T_o - T_w)} \quad \text{eq. 2.9}$$

where for the system water-air (Treybal, 1978):

$$\zeta = \frac{h_g}{\lambda_w} = \frac{950 * k_Y}{\lambda_w} \quad \text{eq. 2.10}$$

The falling rate region starts with a noticeable increase in outlet air temperature and a decrease in the driving force for the water removal. The mass transfer coefficient,  $k_Y a$ , increases which leads to a quicker decrease in the interface moisture content, therefore a decrease in the driving force. Internal diffusion resistance increasingly controls the speed of the drying process which is smaller than the convection process of the constant drying rate. It is assumed that the drying rate in this region is a fraction of that in the constant rate region. This fraction being the ratio of the actual to critical

moisture content ( $w_p/w_c$ ). Lipták *et al.* (1998) presents Shinsky's model (1979) based on equation 2.9 where the differential equation is:

$$m_{wp} dw = \left( \frac{w_p}{w_c} \right) \left( \frac{h_g}{\lambda_w} \right) (T_g - T_w) dA \quad \text{eq. 2.11}$$

Expressing the energy required for evaporation based on temperature drop of the drying gas:

$$\lambda_w m_{wp} dw = \rho Q_a C_p dT \quad \text{eq. 2.12}$$

After solving the differential equation one gets:

$$w_p = \frac{w_c \rho Q_a C_p}{k_y a} \ln \frac{(T_i - T_w)}{(T_o - T_w)} \quad \text{eq. 2.13}$$

Both models depend on the mass transfer coefficient ( $k_y a$ ) which is not constant.

This coefficient depends on both air flow and temperature:

$$k_y a = A Sc^b Re^c \left( \frac{D_{H_2O-air}}{d} \right) \quad \text{eq. 2.14}$$

Where  $A$ ,  $b$ ,  $c$  are adjustable parameters,  $Sc$  is the Schmidt number,  $Re$  is the Reynolds number,  $D_{water-air}$  is the diffusivity and  $d$  is the diameter of the particle. The Schmidt and Reynolds numbers are represented:

$$Sc = \frac{\mu}{\rho D_{H_2O-air}} \quad \text{eq. 2.15}$$

$$Re = \frac{\rho v d_p}{\mu} \quad \text{eq. 2.16}$$

Such correlations are very useful in understanding the phenomena occurring during the drying process. Yet these models lack simplicity at the moment of implementing a control strategy. Both Montenegro and Arocho proposed models that their parameters depend on the region of the curve the process is in and the operating conditions.

Wildfong *et al.* (2002) worked with a different method for drying in a fluid bed dryer. The work done by Wildfong and co-workers was in relation to accelerated fluid bed drying by monitoring the process using a near-infrared spectroscopy. The model developed by Wildfong *et al.* follows the work done by Chandran, Subba and Varma. The difference between both models lies on the definition of the parameters. For the constant rate period, Wildfong's model is as follows:

$$w_p = w_{p_0} - kt \quad \text{eq. 2.17}$$

where, unlike Chandran that describe the  $k$  as drying rate, this constant is described by Wildfong a  
where:

$\rho_g$  = density of the gas

$\rho_s$  = density of the solid

$C_{pg}$  = specific heat capacity of the gas at constant pressure

$T_{inlet}$  = inlet air temperature

$T_{exit}$  = exit air temperature

$H_v$  = latent heat of vaporization

$U_o$  = superficial air velocity measured on an empty chamber

$\epsilon_m$  = void fraction in a packed bed

$L_m$  = bed height

For the falling rate period, Wildfong proposed the following model:

$$w_p = w_p^+ + w_{p_0} ' ke^{-kt} \quad \text{eq. 2.19}$$

where  $w_{p0}'$  is the initial moisture content at the beginning of the falling rate period and  $\kappa$  and  $\kappa'$  are geometric constraints summed over  $n$  terms in an infinite series. This relation can be described by the following formula:

$$w_p = \frac{6}{\pi^2} \left[ \sum_{n=1}^{\infty} \frac{1}{n^2} \exp\left(-n\pi^2 \frac{D_m t}{R^2}\right) \right] (w_{p0}' - w_p^+) + w_p^+ \quad \text{eq. 2.20}$$

where  $D_m$  is the average solvent diffusivity through the particles and  $R$  is the average radius of the particles.

Even though these models describe the drying curve somewhat accurately they possess some limitations in analysis. One of them is applicability. What all of the previous models have in common is the fact that they describe each region of the drying curve separately. This causes a problem for predicting the drying curve, especially if the critical moisture content of a powder is unknown. Applications, like programming, may cause computational error if the critical moisture of a powder is unknown. Another limitation is that being relatively complicated calculations they do not present any attraction for industrial applications.

It is necessary to develop a simple model that is both as practical as an empirical model yet as descriptive and provides understanding of the system and phenomena as a scientific model would be.

## Chapter 3: Materials and Methodology

For the development of the drying curve model the experiment done by Arocho had to be reproduced exactly as it was done by her to compare the model proposed in this work with the model that she developed. The data obtained from the experimentation shall be used to construct a drying curve, analyze the behavior of the drying process, and to develop the parameters of the drying curve model. As it shall be discussed in the following chapter the parameters of the drying curve model depend on operational conditions.

### 3.1 Materials for drying curves experiments

The materials used in the preparation of the pharmaceutical granulation to be dried are included in Table 3.1.

**Table 3.1: List of ingredients for pharmaceutical granulation**

<b>Ingredients</b>	<b>Specification</b>	<b>w/w%</b>
Lactose Monohydrate	Ph. Eur/USP-NF/ JP GranuLac 70 Function: Diluent	80%
Pregelatinized Starch	USP-NF XXIII Colorcon © product 1500 Functions: Diluent, Binder & Desintegrant	13%
Distilled Water	Distilled / pH: 5.50-6.50 Conductivity: 1.8 $\mu\text{s}/\text{cm} \pm (24^{\circ}\text{C})$	7%

### 3.2 Equipment for drying curves experiments

Figure 3.1 shows the schematic diagram of the FBD and the control panel used for drying experiments.

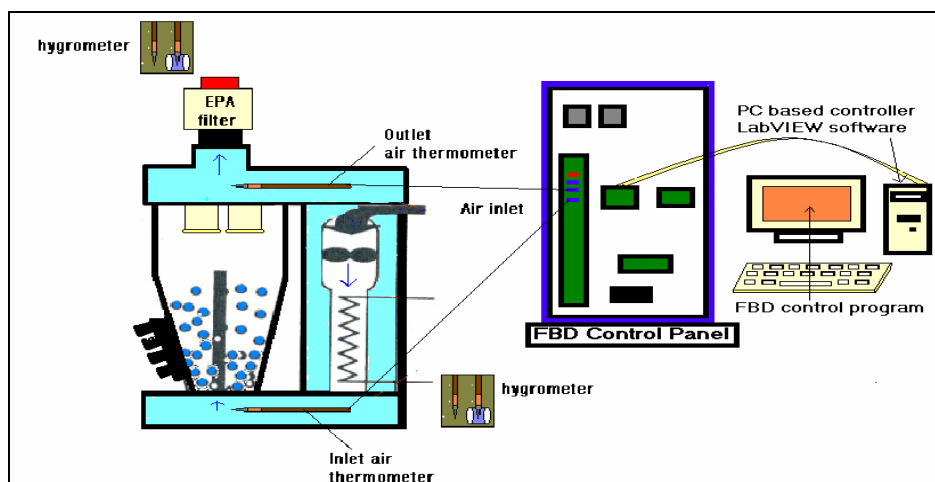


Figure 3.1: Schematics diagram of Fluid Bed Dryer and control panel (Arocho 2004)

Ingredients were weighed in a balance model and mixed in a Littlerford High Shear Mixer with a capacity of 20 kg. The mixer consists of a cylindrical chamber, upper and lower sealed doors, a main shaft with four paddles (two with a shape of V and two near the sidewalls to prevent dead volume), and two motors.

The formulations were dried in a Fluid Bed Dryer Aeromatic AG STREA 1 model shown in Figure 3.1. It consists of a blower with operating conditions between 0-130 m<sup>3</sup>/hr of airflow, an electrical resistance, and a conical recipient bowl with a product container of 16.5 L. The operating temperatures of inlet dry air were in the range of 60 to 100°C. Accessories used were 200 wire mesh product bottom screen, a plate to enhance the fluidization of fine granulations, a 22% free cross sectional air distribution plate with a bypass tube, and nylon T695 exhaust air filters. HEPA filter was placed at the air exit of the equipment.

The samples were analyzed with a Metler Toledo LJ 16 Infrared Moisture Analyzer with a standard balance. The temperature can be programmed from 50 to 160°C. The drying times can be set between 10 to 15 minutes. The drying process can be



controlled automatically and the result is displayed in grams or in terms of mass percent of water removed.

Additional accessories used to conduct the drying curve experiments include Taylor hygrometers to measure dry and wet bulb temperature of the inlet and outlet air, and thermocouples. These were installed at the entrance and exit of air to the product recipient. Thermocouples were type J transition probe ungrounded type Teflon® insulated wires. Temperature ranges for the probes: -100 to 300°C.

### 3.3 Methodology for drying curves experiments

This section is divided into the unit operations used in the experiments and presented in the order they were used.

#### **3.3.1 Powder weighing**

Recipients or containers were thoroughly cleaned and dried before adding the bulk materials. Ingredients for pharmaceutical formulation were weighed. Table 3.1 describes the ingredients used with the specifications and the quantities for the batch size. The ingredients were placed in the Littlerford High Shear Mixer/Granulator after weighing.

#### **3.3.2 Wet granulation preparation**

Before adding the powders, the mixer was thoroughly cleaned and entirely dried prior to starting the mixing operations. The compressed air valve was open until the first flow meter in the rotameter read between 2 and 3 SCFH. Approximately half of the ingredients with a largest quantity in the formulation were added in such a way that it covered the entire mixer's bottom. The complete portion of the remaining ingredients was distributed as evenly as possible on top of the added layer. The remaining half of

ingredients with the largest quantity was added. This is called sandwich addition of the ingredients. Dry mixing was performed for 5 minutes. The mixer was turned off to take a sample for the determination of moisture content. Then the mixer was turned on and the distilled water was added in the provided recipients. The mixing process time continued for 45 minutes. Representative samples of the granulation were taken for analysis of the moisture content with the Moisture Analyzer.

### 3.4 Fluid Bed Drying

Prior to starting drying, the dryer bowl was thoroughly cleaned and dried. The empty dryer bowl was preheated or conditioned until it reached the operational conditions. The wet granulation was divided in recipients of 1 kg each and added to the dryer bowl between consecutive runs. The required devices, inlet and outlet hygrometer were located at the bottom and top of the fluid bed dryer. The operating conditions were described and written in the Fluid Bed Dryer Control Program. Product samples were withdrawn every three minutes. These intervals could change depending on the operating conditions experiment. Airflow velocity and drying temperature were set up depending on the experiment when the drying process was started. Data of inlet and outlet temperatures, wet bulb and dry bulb temperatures were collected during the drying process. When the drying process was finished, the recipient was allowed to cool for 10 to 15 minutes. Then, the dryer bowl was cleaned.

Table 3.2 presents the operating conditions used in the Fluid Bed Dryers. The mass load was 1 kg, the drying temperatures were 60 and 80°C and the AF were between 40 to 80 m<sup>3</sup>/hr. An experimental design was applied to develop the experiments (Montgomery, 1996).

**Table 3.2: Operating conditions used at the FBD**

<b>Air Flow</b>	<b>Mass load</b>	<b>Drying temperature</b>	<b>Initial MC</b>
40 m <sup>3</sup> /hr	1.0 kg	60°C, 80°C	~9.0 %w/w
50 m <sup>3</sup> /hr	1.0 kg	60°C, 80 °C	~9.0 %w/w
60 m <sup>3</sup> /hr	1.0 kg	60°C, 80 °C	~9.0 %w/w
70 m <sup>3</sup> /hr	1.0 kg	60°C, 80 °C	~9.0 %w/w
80 m <sup>3</sup> /hr	1.0 kg	60°C, 80 °C	~9.0 %w/w

### 3.5 LOD Moisture Analyzer

The balance, the printer and the heater were turned on. All aluminum-weighing trays were completely cleaned and dried prior to using. To start with the LOD analysis, the aluminum plate was tared. Between 5.000 and 5.500 g of the samples were weighed. The samples were distributed uniformly in the tray. Temperature was set to 130 °C and the drying time to 15 minutes. Before starting the next analysis, the instrument was allowed to cool down.

## Chapter 4: First Principle Model

### 4.1 Development of the Drying Curve Model

By taking the fluid bed dryer and analyzing the drying process through fundamental energy and mass balances, a practical model for a model predictive control (MPC) algorithm can be obtained. A first assumption is that the drying process is continuous process, which is only true only during operation. This assumption creates a problem since there are no steady state constants in a batch process. In other words what are determined are steady state constants that depend on operating conditions, or pseudo-steady state constants.

The second assumption taken into consideration is that the inlet air humidity is presumed constant. The industry works on a controlled environment so that there is not any source of contamination during production. Another reason for this assumption is that since the experiments were done for a small periods time (15-30 minutes) the changes in inlet air humidity are not significant.

The last assumption used and the most important is that the mass transfer area is not constant and depends on the humidity of the powder. It is commonly presumed that the mass transfer area is constant and is determined as part of the mass transfer coefficient. Yet during the mixing process granulations are generated which creates a wide variety of areas. During the drying process the smallest particles will dry faster than the largest particles. This means that the mass transfer area used at the beginning of the drying process is not the same as the one used at the end of the drying process.

In the dryer there are only two sources of water: air and the powder. A water balance around the powder inside the fluid bed dryer, equation 4.1 is performed to relate the humidity of the pharmaceutical powder to the manipulated variables:

$$m_{\text{pow}} \frac{dw_p(t)}{dt} = -k_y a(t) [Y_{\text{int}}(t) - Y_{\text{air,o}}(t)] \quad \text{eq. 4.1}$$

This mass balance, which can be used for any type of dryer, expresses the negative accumulation of water in the powders as equal to the water removed from it. However, the drying in a FBD occurs fluidizing the powders with inlet airflow which cause an exposure of the entire surface of the powders to the passing air. This causes the smallest particles to dry first and reduces the effective area of mass transfer. Thus,  $a(t)$  in equation 4.1 is a function of the moisture content of powders with a normal particle size distribution. In addition, as the powders get dryer, the outlet temperature of the passing air starts rising which causes the saturation humidity at the inter phase to increase hence  $Y_i(t)$  in equation 4.1 is a function too of the powder moisture content.

The parameter  $k_y$  is a function of the airflow and temperature and  $Y_o(t)$  can be expressed in terms of inlet airflow and temperature as is demonstrated below. For this, a water balance on the air describing the effect of the drying process on the environment is performed:

$$\underbrace{V \frac{d(\rho_{\text{air,o}}(t) Y_{\text{air,o}}(t))}{dt}}_{\text{Accumulated water}} = \underbrace{\rho_{\text{air,i}}(t) q_{\text{air,i}}(t) Y_{\text{air,i}}}_{\text{Inlet water flow}} - \underbrace{\rho_{\text{air,o}}(t) q_{\text{air,o}}(t) Y_{\text{air,o}}(t)}_{\text{Output water flow}} + \underbrace{k_y(t) a(t) [Y_{\text{int}}(t) - Y_{\text{air,o}}(t)]}_{\text{Water removed from powder by drying}} \quad \text{eq. 4.2}$$

where:

$k_y a(t)$ : Mass transfer coefficient [kg of dry air/s]

$Y_{\text{int}}(t)$ : Inter phase humidity [kg water/kg of dry air]

$Y_{\text{air}}(t)$ : Air humidity [kg water/kg of dry air]

$\rho_{\text{air}}(t)$ : Air density [kg air/L]

$V$  : Volume of air in the dryer [L]

$q_{\text{air}}$ : Air flow [m<sup>3</sup>/hr]

By examining equation 4.2, it can be concluded that the air water content depends on the temperature and airflow rate. Then, to eliminate the dependence with the outlet conditions, a total mass balance for the air, equation 4.3, is made to relate the output variables in equation 4.2 to the input variables:

$$V \frac{d\rho_{\text{air,o}}(t)}{dt} = \rho_{\text{air,i}}(t)q_{\text{air,i}}(t) - \rho_{\text{air,o}}(t)q_{\text{air,o}}(t) \quad \text{eq. 4.3}$$

Expressing the air's density based on temperature, doing some linearization, transforming equation 4.2 using Laplace and doing some algebra it gets reduced to the following equation:

$$\Gamma_{\text{o,m}}(s) = \frac{K_{\text{m2,1}}}{\tau_{\text{m2}}s + 1} Q_{\text{air,i}}(s) + \frac{K_{\text{m2,2}}}{\tau_{\text{m2}}s + 1} \Gamma_{\text{i}}(s) - \frac{K_{\text{m2,3}}}{\tau_{\text{m2}}s + 1} Q_{\text{air,o}}(s) \quad \text{eq. 4.4}$$

By making a global energy balance around the air the output temperature can also be related to the airflow and input temperature:

$$V \underbrace{\frac{d[\rho_{\text{air,o}}(t)T_{\text{o}}(t)Cp_{\text{o}}(t)]}{dt}}_{\text{Accumulated energy in air}} = \underbrace{q_{\text{air,i}}(t)\rho_{\text{air,i}}(t)T_{\text{i}}(t)Cp_{\text{i}}(t)}_{\text{Inlet energy in air}} - \underbrace{q_{\text{air,o}}(t)\rho_{\text{air,o}}(t)T_{\text{o}}(t)Cp_{\text{o}}(t)}_{\text{Outlet energy in air}} \quad \text{eq. 4.5}$$

where :

$Cp_{\text{i}}(t)$  : Heat capacity of inlet air at constant pressure [J/°C · s]

$Cp_{\text{o}}(t)$  : Heat capacity of outlet humid air at constant pressure [J/°C · s]

$T(t)$  : Air temperature [°C]

After following the same procedure to obtain equation 4.4, equation 4.5 is reduced to:

$$\Gamma_{o,E}(s) = \frac{K_{EI,1}}{\tau_{EI}s+1} Q_{air,i}(s) + \frac{K_{EI,2}}{\tau_{EI}s+1} \Gamma_i(s) - \frac{K_{EI,3}}{\tau_{EI}s+1} Q_{air,o}(s) - \frac{K_{EI,4}(\tau_{1_{EI}}s+1)}{\tau_{EI}s+1} \hat{Y}_{air,o}(s) \quad \text{eq. 4.6}$$

Equations 4.4 and 4.6 relate the output temperature to the input temperature and airflow and the output airflow. Since the value of this output temperature does not depend on which type of balance used then that means that equation 4.4 and 4.6 are equal. By equating both equations the output airflow is related to the input variables as follows:

$$Q_{air,o}(s) = \frac{K_{q1}(\tau_{lq0,1}s+1)}{\tau_{q0}s+1} Q_{air,i}(s) + \frac{K_{q2}(\tau_{lq0,2}s+1)}{\tau_{q0}s+1} \Gamma_i(s) - \frac{K_{q3}(\tau_{lq0,3}s+1)(\tau_{1_{EI}}s+1)}{\tau_{q0}s+1} \hat{Y}_{air,o}(s) \quad \text{eq. 4.7}$$

By combining eq. 4.7 and equation 4.6, this equation is reduced to:

$$\Gamma_o(s) = \frac{K_{T1}(\tau_{IT1}s+1)}{(\tau_{q0}s+1)(\tau_{EI}s+1)} Q_{air,i}(s) + \frac{K_{T2}(\tau_{IT2}s+1)}{(\tau_{q0}s+1)(\tau_{EI}s+1)} \Gamma_i(s) - \frac{K_{T3}(\tau_{lq0,2}s+1)(\tau_{1_{EI}}s+1)}{(\tau_{q0}s+1)(\tau_{EI}s+1)} \hat{Y}_{air,o}(s) \quad \text{eq. 4.8}$$

Equations 4.7 and 4.8 relate output temperature and output air flow to the input airflow and temperature. Now that all the output operating variables (temperature and airflow) are related to the desired manipulated variables (input temperature and airflow), the observable variables (output air humidity and inter phase humidity) are to be related to these variables. An energy balance around the powder is the first stepping stone towards this goal:

$$m_{pow} C_{p,pow} \frac{dT_s(t)}{dt} = U(t)A[T_o(t) - T_s(t)] \quad \text{eq. 4.9}$$

where :

$m_{\text{pow}}$  : Mass of Powder [kg]

$C_{p_{\text{pow}}}(t)$  : Heat capacity of powder at constant pressure [J/°C · s]

$U(t)$  : Overall heat transfer coefficient [J/m<sup>2</sup> · °C · s]

$A$  : Area perpendicular to heat flow [m<sup>2</sup>]

$T(t)$  : Air temperature [°C]

$T_s(t)$  : Saturation temperature at inter phase [°C]

After transforming equation 4.9 using Laplace transformation, performing a linearization, and combining it with equation 4.8, the solution is:

$$\Gamma_s(s) = \frac{K_{E2,1}(\tau_{IE2,1}s+1)(\tau_{IE2,2}s+1)}{(\tau_{q0}s+1)(\tau_{m2}s+1)(\tau_{E2}s+1)} Q_{\text{air},i}(s) + \frac{K_{E2,1}(\tau_{IE2,3}s+1)(\tau_{IE2,4}s+1)}{(\tau_{q0}s+1)(\tau_{m2}s+1)(\tau_{E2}s+1)} \Gamma_i(s) + \frac{K_{E2,3}(\tau_{Iq0,3}s+1)(\tau_{IE1}s+1)}{(\tau_{q0}s+1)(\tau_{m2}s+1)(\tau_{E2}s+1)} \hat{Y}_{\text{air},o}(s) \quad \text{eq. 4.10}$$

Combining equations 4.7, 4.8 and 4.10 with equation 4.2 and using a Taylor approximation the expression that appears is:

$$\hat{Y}_{\text{air},o}(s) \approx \frac{k_{Y,Q}^{\text{eff}} e^{-\theta_{y1}s}}{(\tau_q^{\text{eff}} s+1)} Q_{\text{air},i}(s) + \frac{k_{Y,\Gamma}^{\text{eff}} e^{-\theta_{y2}s}}{(\tau_q^{\text{eff}} s+1)} \Gamma_i(s) + \frac{k_{Y,W_p}^{\text{eff}} e^{-\theta_{y3}s}}{(\tau_q^{\text{eff}} s+1)} W_p(s) \quad \text{eq. 4.11}$$

Once equation 4.11 is introduced to equation 4.1 and combined with the previous equations and Laplace transformation, and implementing a Taylor series expansion the relationship between the moisture content of the powder and the inlet temperature and air flow is as follows:

$$W_p(s) = \frac{-K_q e^{-\theta_1 s}}{\tau_s + 1} Q_{\text{air},i}(s) - \frac{K_t e^{-\theta_2 s}}{\tau_s + 1} T_i(s) \quad \text{eq. 4.12}$$

## 4.2 First Principle Model Results



Equation 4.12 described an approximate solution to the water mass balance around the powder, giving a relationship between the inlet airflow and temperature, the two desired control parameters. After observing the drying curves of the placebo the solution of a step response of both airflow and temperature for equation 4.12 in the time dimension is as follows:

$$\Delta W_p(t) = \left( Kq\Delta Q_{air,i}(t) + Kt\Delta T_i(t) \right) \left( 1 - e^{-\frac{t}{\tau}} \right) \quad \text{eq. 4.13}$$

As said before, the parameters of equation 4.13 are dependent of operational conditions, since in a continuous process these parameters would be the steady state parameters. The values of these parameters at different inlet temperatures and airflows are as follow:

**Table 4.1: Values of Kq at different operational conditions**

<b>Kq</b>	<b><math>\Delta T = 35 \text{ }^\circ\text{C}</math></b>	<b><math>\Delta T = 55 \text{ }^\circ\text{C}</math></b>
40 m <sup>3</sup> /hr	-0.055	-0.035
50 m <sup>3</sup> /hr	-0.06	-0.053
60 m <sup>3</sup> /hr	-0.05	-0.03
70 m <sup>3</sup> /hr	-0.05	-0.03
80 m <sup>3</sup> /hr	-0.04	-0.041

**Table 4.2: Values of Kt at different operational conditions**

<b>Kt</b>	<b><math>\Delta T = 35 \text{ }^\circ\text{C}</math></b>	<b><math>\Delta T = 55 \text{ }^\circ\text{C}</math></b>
40 m <sup>3</sup> /hr	-0.06	-0.046
50 m <sup>3</sup> /hr	-0.049	-0.05
60 m <sup>3</sup> /hr	-0.04	-0.04
70 m <sup>3</sup> /hr	-0.05	-0.04
80 m <sup>3</sup> /hr	-0.04	-0.026

**Table 4.3: Values of  $\tau$  at different operational conditions**

$\tau$	$\Delta T = 35\text{ }^{\circ}\text{C}$	$\Delta T = 55\text{ }^{\circ}\text{C}$
40 m <sup>3</sup> /hr	0.29	0.29
50 m <sup>3</sup> /hr	0.1	0.1
60 m <sup>3</sup> /hr	0.1	0.1
70 m <sup>3</sup> /hr	0.1	0.08
80 m <sup>3</sup> /hr	0.06	0.05

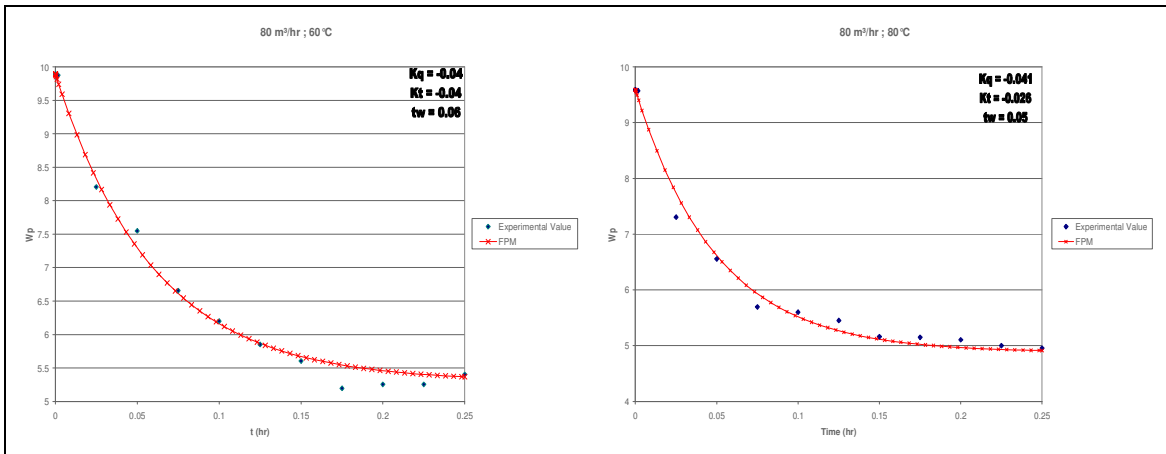


Figure 4.1: Prediction of drying curve using First Principle Model at airflow of 80 m<sup>3</sup>/hr and operating temperatures of 60 °C ( $\Delta T = 35^{\circ}\text{C}$ ) and 80 °C ( $\Delta T = 55^{\circ}\text{C}$ )

**Table 4.4:  $R^2$  and standard deviation of the FPM at different operating conditions**

Airflow and Temperature	$R^2$	$\sigma^2$
40 m <sup>3</sup> /hr ; 60 °C	0.98	0.013
40 m <sup>3</sup> /hr ; 80 °C	0.98	0.014
50 m <sup>3</sup> /hr ; 60 °C	0.94	0.039
50 m <sup>3</sup> /hr ; 80 °C	0.83	0.10
60 m <sup>3</sup> /hr ; 60 °C	0.98	0.012
60 m <sup>3</sup> /hr ; 80 °C	0.98	0.013
70 m <sup>3</sup> /hr ; 60 °C	0.98	0.010
70 m <sup>3</sup> /hr ; 80 °C	0.94	0.034
80 m <sup>3</sup> /hr ; 60 °C	0.96	0.026
80 m <sup>3</sup> /hr ; 80 °C	0.95	0.032

At operating conditions of 40 m<sup>3</sup>/hr and 60°C the model proposed by Arocho (2004) failed to describe the final minutes of the drying process, while the first principle model (FPM) managed to describe the entire curve as seen on Figure 4.2.

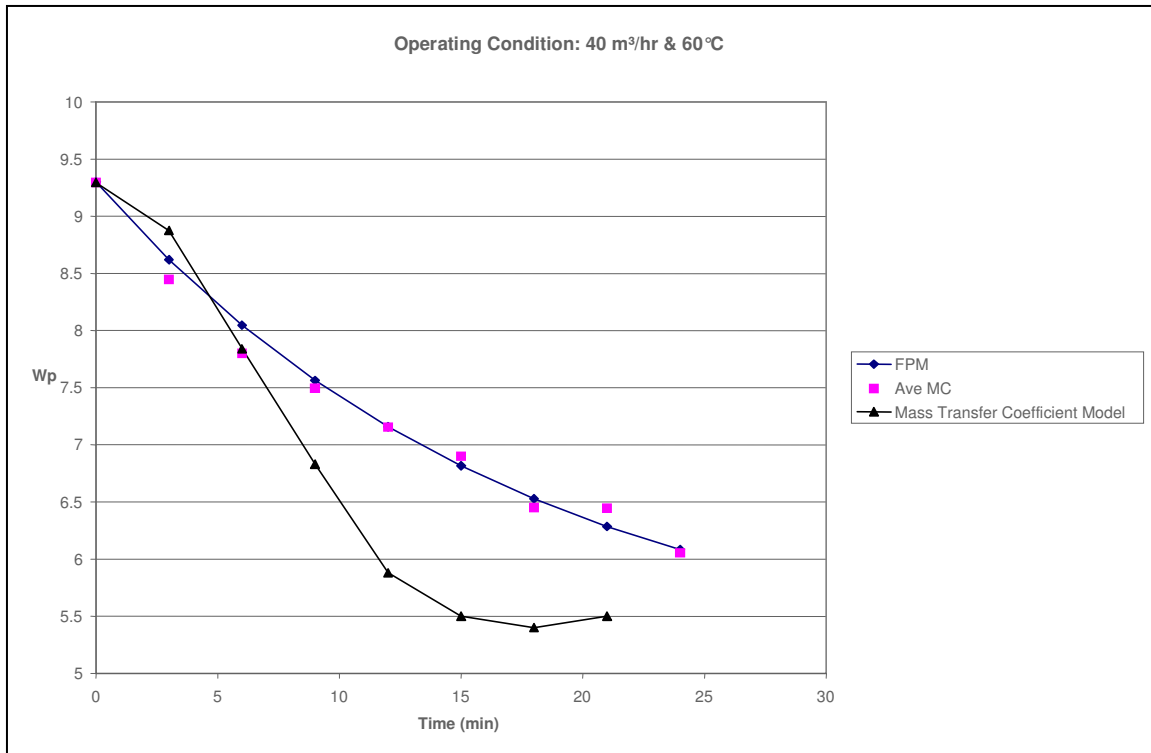


Figure 4.2: Comparison between the models using the Mass Transfer Coefficient and the FPM

The FPM model describes the drying curve better than the correlation proposed by Arocho, but the parameters do not represent physical conditions. Through the reductions and linearization done to obtain the FPM the physical meaning of the parameters are lost. If the desire is to study and understand the phenomena behind the drying process the model proposed by Arocho provides with such an understanding of the behavior. On the other hand if a macro study of the drying process is enough the FPM develops precisely the drying curve. Having a model that can describe the drying curve of a pharmaceutical powder (with precision and being a simpler model than the other models proposed) the design of a MPC strategy can then be developed.

## Chapter 5: Development of the Model Predictive Controller

### 5.1 MPC Design

The MPC strategy is based on the idea of determining changes on the manipulated variables based on a predicted trajectory of the process. Such changes are calculated in the control block of the strategy (see figure 2.1). The calculations made by the controller are to determine the optimum input changes required to minimize the objective function (equation 2.1). This equation can be written in matrix form as:

$$J = E(k+1)^T Q E(k+1) + \Delta U(k)^T R \Delta U(k) \quad \text{eq. 5.1}$$

Where  $E$  is the error between a reference trajectory and the model trajectory,  $\Delta U$  is the trajectory of input changes, and  $Q$  and  $R$  are weight matrixes.

Equation 4.13 can be written in matrix form too if the maximum acceptable drying time is known:

$$\hat{W}_p(k+1) = K \Delta U(k) + \hat{W}_p(k) \quad \text{eq. 5.2}$$

$$\text{where } K = \begin{bmatrix} K_1 & 0 & \dots & 0 \\ 0 & K_2 & \ddots & \vdots \\ 0 & \ddots & \ddots & 0 \\ \vdots & \ddots & 0 & K_M \\ \vdots & \dots & \vdots & \vdots \\ 0 & \dots & 0 & K_P \end{bmatrix}$$

$$K_i = \left( 1 - e^{-\frac{k_i}{\tau}} \right) \begin{bmatrix} K_q & K_t \end{bmatrix}$$

$$\Delta U(k) = [\mathbf{u}(k), \mathbf{u}(k+1), \dots, \mathbf{u}(k+M-1)]^T$$

$$\mathbf{u} = [\Delta Q_{\text{air},i} \quad \Delta T_i]$$

When introducing equation 5.2 into equation 5.1 and minimizing the objective function, the solution is:

$$\Delta U(k) = \left( \mathbf{K}^T \mathbf{Q} \mathbf{K} + \mathbf{R} \right)^{-1} \mathbf{K}^T \mathbf{Q} \hat{\mathbf{E}}^o(k+1) = \mathbf{K}_c \hat{\mathbf{E}}^o(k+1) \quad \text{eq. 5.3}$$

where  $\hat{\mathbf{E}}^o(k+1)$  is the error between the reference and the predicted trajectory.

In equation 5.2, the  $\mathbf{K}$  matrix is a  $2M \times P$  matrix,  $\mathbf{Q}$  is a  $P \times P$  weight matrix related to the output changes and  $\mathbf{R}$  is a  $2M \times 2M$  matrix related to the input changes.  $M$  is known as the control horizon which is the manipulated input changes in which the predicted response moves to the set point.  $P$  is the prediction horizon which is the number of predictions of the process. Dougherty and Cooper (2002) developed a series of relationships between the process model and the values of  $M$ ,  $P$ , and the elements of  $\mathbf{Q}$  and  $\mathbf{R}$ :

**Table 5.1: Relationships between the process model and MPC parameters.**  
 $\gamma_r^2$  is the diagonal element of  $\mathbf{Q}$  and  $\lambda_s^2$  is the diagonal element of  $\mathbf{R}$ .

Non-adaptive DMC tuning strategy
1. Approximate the process dynamics of all controller output to measured process variable pairs with FOPDT models: $\frac{y_r(s)}{u_s(s)} = \frac{K_{rs} e^{-\theta_{rs} s}}{\tau_{rs} s + 1} \quad (r = 1, 2, \dots, R; s = 1, 2, \dots, S)$
2. Select the sample time as close as possible to: $T_{rs} = \text{Max}(0.1\tau_{rs}, 0.5\theta_{rs}),$ $(r = 1, 2, \dots, R; s = 1, 2, \dots, S)$ $T = \text{Min}(T_{rs}),$
3. Compute the prediction horizon, $P$ , and the model horizon, $N$ : $P = N = \text{Max}\left(\frac{5\tau_{rs}}{T} + k_{rs}\right) \quad \text{where } k_{rs} = \left(\frac{\theta_{rs}}{T} + 1\right) \quad (r = 1, 2, \dots, R; s = 1, 2, \dots, S)$
4. Compute a control horizon, $M$ : $M = \text{Max}\left(\frac{\tau_{rs}}{T} + k_{rs}\right) \quad (r = 1, 2, \dots, R; s = 1, 2, \dots, S)$
5. Select the controlled variable weights, $\gamma_r^2$ , to scale process variable units to be the same.
6. Compute the move suppression coefficients, $\lambda_s^2$ : $\lambda_s^2 = \frac{M}{10} \sum_{r=1}^R \left[ \gamma_r^2 K_{rs}^2 \left\{ P - k_{rs} - \frac{3\tau_{rs}}{2T} + 2 - \frac{(M-1)}{2} \right\} \right] \quad (s = 1, 2, \dots, S)$
7. Implement DMC using the traditional step response matrix of the actual process and the initial values of the parameters computed in steps 1-6.

Following this series of relationship, the initial values the parameters are:

**Table 5.2: Initial values of MPC parameters**

<b>M</b>	22
<b>P</b>	51
$\gamma_r^2$	1
$\lambda_{s,1}^2$	0.06092
$\lambda_{s,2}^2$	0.02879

After a tuning process done by trial and error the final values of these parameters used for the simulation are:

**Table 5.3: Final values of the MPC parameters**

<b>M</b>	22
<b>P</b>	51
$\gamma_r^2$	0.3
$\lambda_{s,1}^2$	2.4368e-05
$\lambda_{s,2}^2$	1.1516e-05

## 5.2 Simulation Result

By using these values for the design of the MPC strategy a program written in MATLAB® was used to simulate the response of the drying process to the control strategy. For simulation purposes the drying curve model determined in chapter 3 was used to simulate the fluid bed dryer. The process model used both for the prediction and to represent the drying process in this simulation was a constant-parameter model determined after examination of the behavior of the drying curve model. The response of this simulation is shown in the following figure:

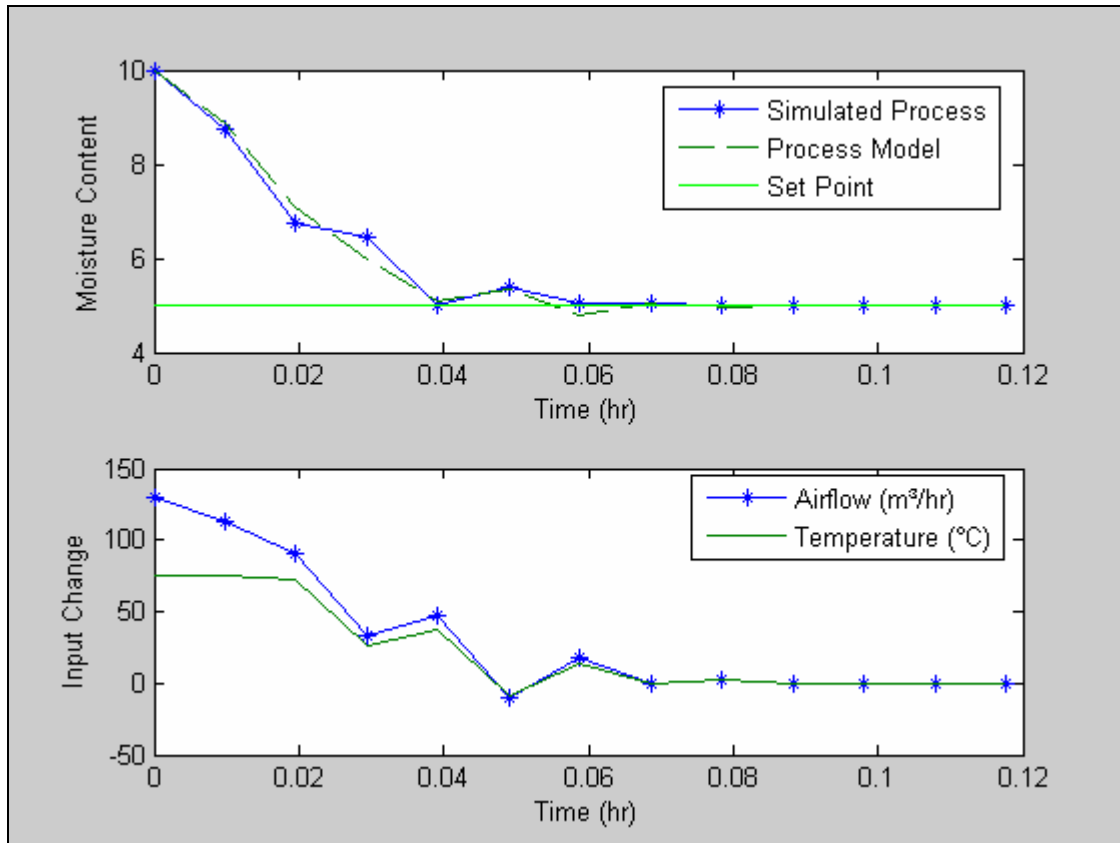


Figure 5.1: Process response of the fluid bed dryer after implementing an MPC algorithm

As can be seen, there are 2 relevant features. First, both manipulated variables start at their maximum values permitted. However, as the powders start drying, both variables start decreasing until they come to a leveled value. This behavior agrees with the known phenomena occurring during that window of time which are mass and energy transfer by convection and diffusion. The drying starts with a high convection to favor the mass and energy balance and decrease to low flows and temperature since the diffusion would not be increased dramatically specially with high flows.

The operational reduction at every sampling time obtained from implementing the MPC strategy is determined in the following table. The reduction in operational conditions indicates a reduction of operational costs since the equipment work most of the time at minimum capacity and the drying time is reduced.

**Table 5.4: Comparison between operational monitoring done by the MPC and an operator for airflow changes.**

<b>Airflow Change Calculated by MPC</b>	<b>Airflow Change Commonly Used</b>	<b>Percentage of Reduction</b>
130	130	0
113.54	130	12.66
90.274	130	30.56
33.045	130	74.58
46.757	130	64.03
-10.258	130	107.89
17.28	130	86.71
0.10533	130	99.91
2.3309	130	98.21
0.22319	130	99.82
0.1829	130	99.86
0.0035275	130	100
0.0075515	130	100

**Table 5.5: Comparison between operational monitoring done by the MPC and an operator for temperature changes**

<b>Temperature Change Calculated by MPC</b>	<b>Temperature Change Commonly Used</b>	<b>Percentage of Reduction</b>
75	75	0
75	75	0
72.219	75	3.708
26.436	75	64.752
37.406	75	50.13
-8.2065	75	110.94
13.824	75	81.57
0.084264	75	99.89
1.8647	75	97.51
0.17855	75	99.76
0.14632	75	99.80
0.002822	75	100
0.0060412	75	100



### 5.3 Stability Test for the MPC

The General Stability Criterion says that “a feedback control system is stable if and only if all roots of the characteristic equation lie to the left of the imaginary axis in the complex plane”. The characteristic equation of a feedback control system is defined as:

$$1 + G_{OL} = 0 \quad \text{eq. 5.4}$$

where the open-loop transfer function is  $G_{OL}(s) = G_C(s)G_V(s)G_P(s)G_M(s)$  (the transfer functions of the controller, valve, process and the transmitter respectively). By using a root locus (Figure 5.2) it can be shown how the characteristic equation changes as the controller gain  $K_C$  changes. The roots of the characteristic equation are the values of the complex variables that satisfy equation 5.4. Thus each point on the root locus satisfies the following equation, a rearrangement of equation 5.4:

$$G_{OL}(s) = -1 \quad \text{eq. 5.5}$$

The corresponding magnitude and argument are:

$$|G_{OL}(j\omega)| = 1 \text{ and } \angle G_{OL}(j\omega) = -180^\circ \quad \text{eq. 5.6}$$

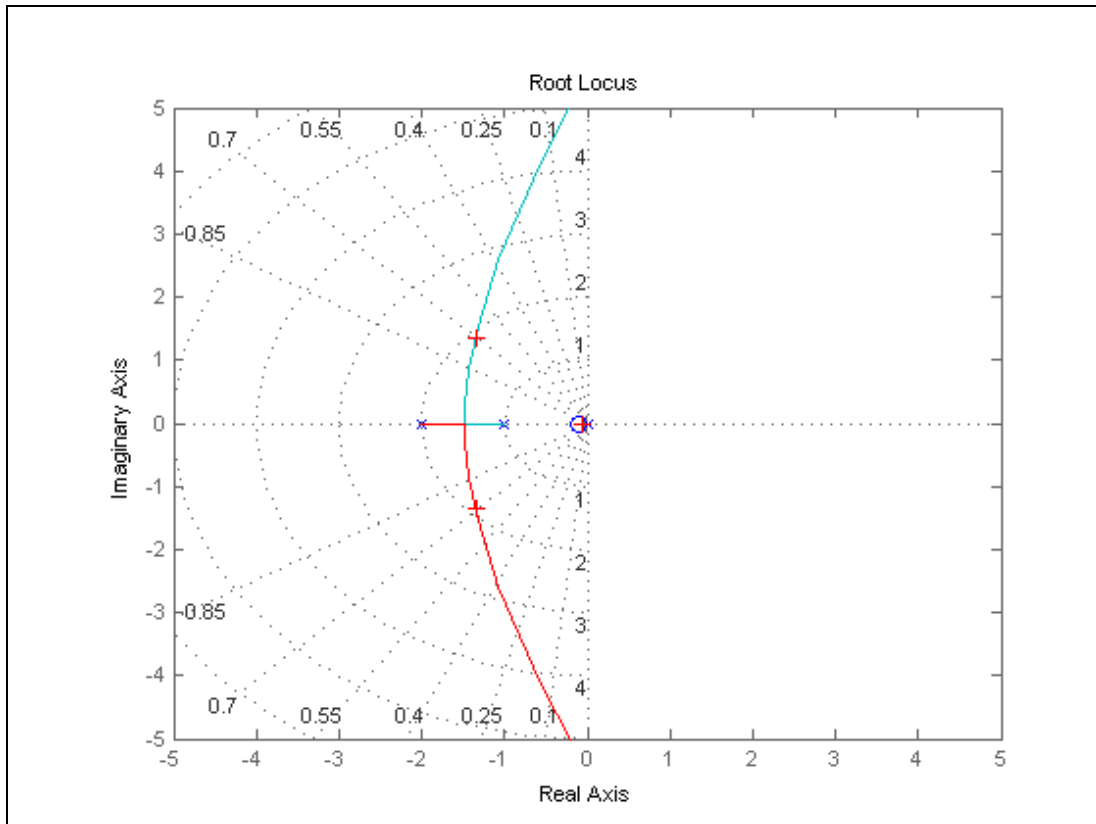


Figure 5.2: Example of a root locus plot.

In general the  $i$ th root of the characteristic equation can be expressed as a complex number,  $r_i = a_i \pm b_i j$ . When a pair is located on the imaginary axis, the real part is zero and the closed-loop system is at the stability limit. This condition is referred to as marginal stability. For a marginally stable system with  $b_i \neq 0$ , the frequency of the sustained oscillation,  $\omega_C$ , is given by  $\omega_C = b_i$ . This oscillatory behavior is caused by the pair of the roots on the imaginary axis at  $s = \pm \omega_C j$ . Substituting this expression for  $s$  into equation 5.6 gives the following expressions for a conditionally stable system:

$$AR_{OL}(\omega_C) = |G_{OL}(j\omega_C)| = 1 \quad \text{eq. 5.7}$$

$$\Phi_{OL}(\omega_C) = \angle G_{OL}(j\omega_C) = -180^\circ \quad \text{eq. 5.8}$$

for some particular value of  $\omega_C > 0$ . The critical frequency  $\omega_C$  is defined to be a value of  $\omega$  for which  $\Phi_{OL}(\omega) = -180^\circ$  and, for a marginally stable system,  $AR_{OL}(\omega) = 1$

The Bode Stability Criterion states that for an open-loop transfer function that is strictly proper (more poles than zeros) and has no poles located on or to the right of the imaginary axis, with the possible exception of a single pole at the origin, if the function has a single critical frequency, then the closed-loop system is stable if  $AR_{OL}(\omega_C) < 1$ . Otherwise the system is unstable. In other words, to determine the value for the control gain that makes the system stable it is necessary to examine at what value of  $K_C$  makes the system reach the critical frequency, also known as the ultimate gain.

In the following Figure it is shown a Bode plot of the drying curve model (presuming that the valve and transmitter functions are equal to 1) with constant parameters. The plots show that the curve never reaches a phase value of  $-180^\circ$ . As a matter of fact the curve is asymptotic at  $90^\circ$ . Since the critical frequency is never reached then there is no ultimate gain. In other words the process is stable at any control gain ( $K_C$ ) that it is used.

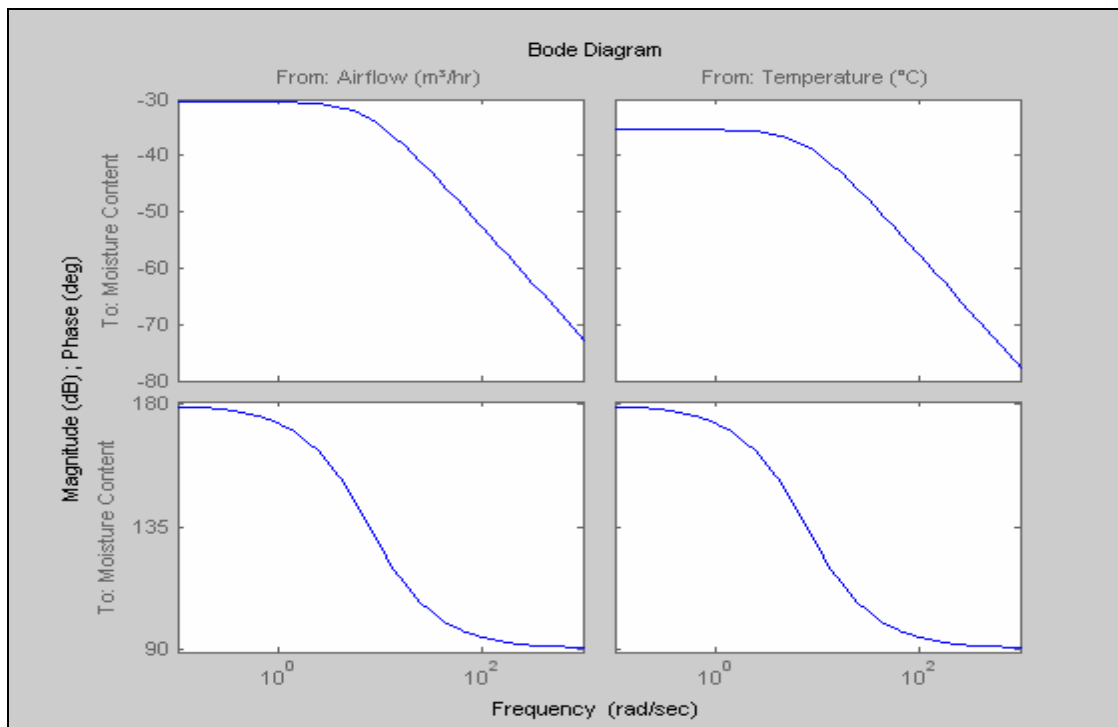


Figure 5.3: Bode Diagram for the MPC design using the Drying Curve Model with constant parameters.

## Chapter 6: Other Approaches to MPC Design

In the Chapter 5 it was developed a MPC strategy algorithm for the drying process of pharmaceutical powders in a fluid bed dryer. The simulation of this strategy has proven an optimization in operational input and in drying time. The MPC strategy developed follows the flow chart presented in Figure 2.3, but the calculations made do not follow any conventional method presented in the literature. In this chapter the MPC strategy developed in the previous chapter will be compared to conventional MPC strategies presented in literature and commercial toolboxes. For this study the process model shall be represented by the model with constant parameters:

$$W_p(s) = \frac{-0.03}{0.035s + 1} Q(s) + \frac{-0.015}{0.035s + 1} \Gamma(s) \quad \text{eq. 6.1}$$

### 6.1 Step-response MPC

Step-response models offer the advantage that they can represent stable processes with unusual dynamic behavior that cannot be accurately described by simple transfer function models. Their main disadvantage is the large number of model parameters. Although step-response models are not suitable for unstable processes, they can be modified to represent integrating processes. This model can be expressed as follows:

$$y(k+1) = y_0 + \sum_{i=1}^{N-1} S_i \Delta u(k-i+1) + S_N u(k-N+1) \quad \text{eq. 6.2}$$

where  $y(k+1)$  is the output variable at the  $(k+1)$  sampling instant, and  $\Delta u(k-i+1)$  denotes the change in the manipulated input from one sampling instant to the next,  $\Delta u(k-i+1) = u(k-i+1) - u(k-i)$ . Both  $y$  and  $u$  are deviation variables. The model

parameters are the N step-response coefficients,  $S_1$  to  $S_N$ . Typically, N is selected so that  $30 \leq N \leq 120$ . The initial value  $y(0)$  is denoted by  $y_0$ .

Equation 6.2 also represents one-step-ahead prediction of the process. For a two-step-ahead prediction the step-response model is as follows:

$$y(k+2) = \underbrace{S_1 \Delta u(k+1)}_{\text{Future control move}} + \underbrace{S_2 \Delta u(k)}_{\text{Current control action}} + \underbrace{\sum_{i=3}^{N-1} S_i \Delta u(k-i+1) + S_N u(k-N+1)}_{\substack{\text{Past control action} \\ \text{Predicted unforced response}}} \quad \text{eq. 6.3}$$

Following an analogous method used for equation 6.3, for a P-step-ahead prediction the model looks like:

$$y(k+P) = \underbrace{\sum_{i=1}^P S_i \Delta u(k+P-i)}_{\substack{\text{Effect of current and} \\ \text{future control actions}}} + \underbrace{\sum_{i=P+1}^{N-1} S_i \Delta u(k+P-i) + S_N u(k+P-N)}_{\substack{y^0(k+P) \\ \text{Effect of past control actions} \\ \text{Predicted unforced response}}} \quad \text{eq. 6.4}$$

Equation 6.4 can be written in matrix form:

$$\hat{Y}(k+1) = S \Delta U(k) + Y^0(k+1) \quad \text{eq. 6.5}$$

For a more precise model a corrected version of equation 6.5 is presented as followed. In this equation the error between the model and the process is present to correct for any disturbance in the process:

$$\tilde{Y}(k+1) = S \Delta U(k) + \hat{Y}^0(k+1) + \left[ y(k) - \hat{y} \right] I \quad \text{eq. 6.6}$$

where :

$$\begin{aligned}\tilde{Y}(k+1) &= [\tilde{y}(k+1), \tilde{y}(k+2), \dots, \tilde{y}(k+P)]^T \\ U(k) &= [u(k), u(k+1), \dots, u(k+M-1)]^T \\ \hat{Y}^0(k+1) &= \left[ \tilde{y}^0(k+1), \tilde{y}^0(k+2), \dots, \tilde{y}^0(k+P) \right]^T \\ S &= \begin{bmatrix} S_1 & 0 & \dots & 0 \\ S_2 & S_1 & 0 & \vdots \\ \vdots & \vdots & \ddots & 0 \\ S_M & S_{M-1} & \dots & S_1 \\ S_{M+1} & S_M & \dots & S_2 \\ \vdots & \vdots & \vdots & \vdots \\ S_P & S_{P-1} & \dots & S_{P-M+1} \end{bmatrix}\end{aligned}$$

where the elements of the S matrix are the gains of the process when the input changes are equal to unity and reaches steady state.

The prediction model used to determine the error between the set point and the process trajectory is as follow:

$$\hat{Y}^0(k+1) = S^* \Delta U(k) + M Y^0(k) \quad \text{eq. 6.7}$$

where :

$$\begin{aligned}\hat{Y}^0(k) &= \left[ \tilde{y}^0(k), \tilde{y}^0(k+1), \dots, \tilde{y}^0(k+P-1) \right]^T \\ M &= \begin{bmatrix} 0 & I & 0 & \dots & 0 \\ 0 & 0 & I & \ddots & 0 \\ \vdots & \vdots & \vdots & \ddots & 0 \\ 0 & 0 & \dots & 0 & I \\ 0 & 0 & \dots & 0 & I \end{bmatrix} \\ S^* &= \begin{bmatrix} S_1 \\ S_2 \\ \vdots \\ S_{P-1} \\ S_P \end{bmatrix}\end{aligned}$$

The basis of the MPC strategy is to optimize the objective function (equation 2.14). For the step-response model the solution to the optimization of the objective function is as follows:

$$\Delta U(k) = \left( K^T Q K + R \right)^{-1} K^T Q \hat{E}^o(k+1) = K_c \hat{E}^o(k+1) \quad \text{eq. 6.8}$$

This equation, equivalent to equation 5.3 but with different matrix formation, is the control basis in the MPC strategy. The definition of the weight matrixes Q and R are the same as given in the previous chapter.

The simulation of this MPC strategy is shown in the following Figure:

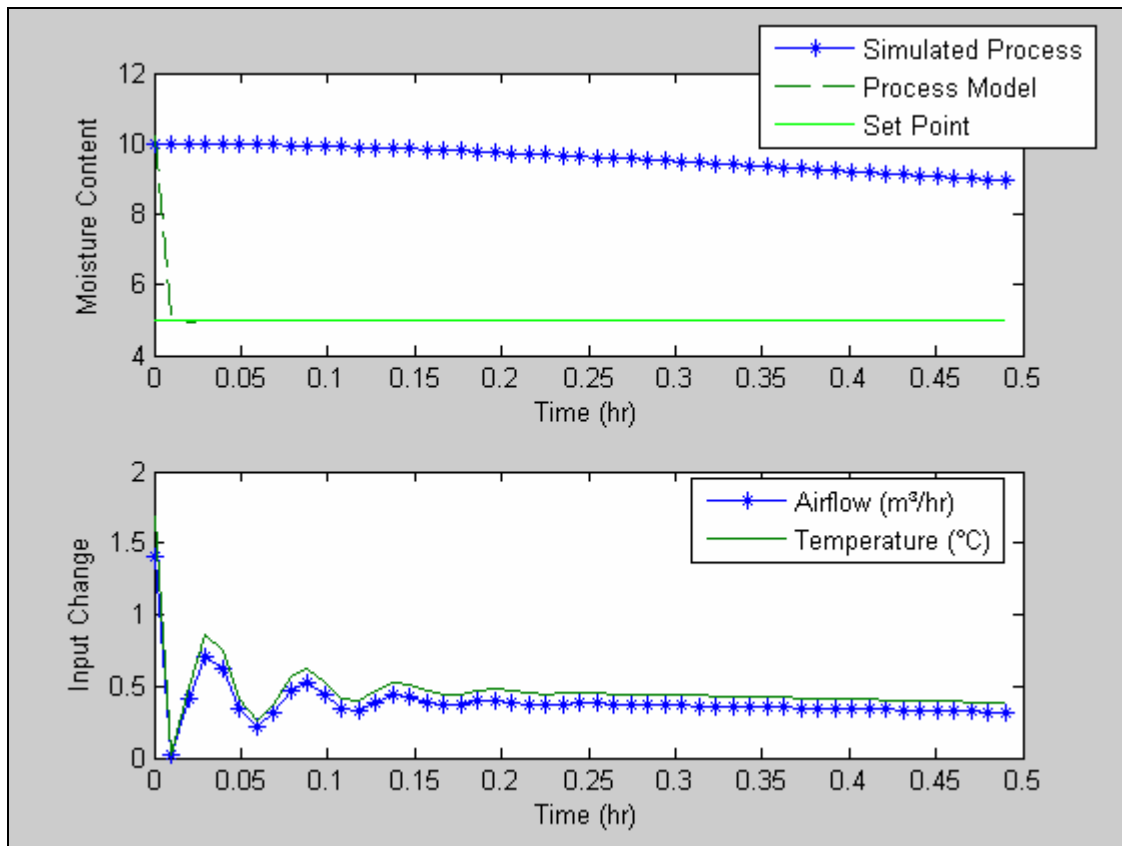


Figure 6.1: Process response of the fluid bed dryer after implementing step-response MPC algorithm.

The process model does not represent in any way the true behavior of the drying process in a fluid bed dryer, as shown in figure 4. The step-response model is constructed by an analysis of the response of the process when the input changes are equal to unity. By allowing a unit input change the process gain can be analyzed with the assurance that immeasurable disturbances affect the behavior of the process. In the drying process no matter the operational conditions, if the starting humidity is constant for every possible operating condition, the process gain will always be the same. The difference between operating conditions lies on the drying time. Since the drying time is fixed for one type of operating conditions the calculations made by the controller are based on this provided information. This allowed for the controller to presume that changes were being made by the process when what actually happened was that the process was maintained constant.

The behavior of the input change does not respond as it would be expected by any control strategy. The maximum capacity of the machine is never reached. The precision of the prediction model is very important, as seen in this example. Because of the process model's lack of accuracy, the input changes calculated are not reasonable and does not allow for the drying process to be executed as it should be.

## 6.2 State-space MPC

In the *state-space* analysis there are three types of variables that are involved in the modeling of dynamic system: input, output and state variables. The state variables of a dynamic system are the variables making up the smallest set of variables that determine the state of the dynamic system. The state-space representation for a system is not unique, except that the number of state variables is the same for any of the different state-space



representations. Any set of transfer functions of any system can be represented in state-space by the following form (Valencia, 2005):

$$\begin{aligned} \dot{x}(t) &= Ax(t) + Bu(t) \\ y(t) &= Cx(t) + Du(t) \end{aligned} \quad \text{eq. 6.9}$$

where  $A$  is called the state matrix,  $B$  the input matrix,  $C$  the output matrix,  $D$  the direct transmission matrix,  $u(t)$  the control vector,  $x(t)$  the state vector and  $y(t)$  the output vector.

Based on equation 6.1 the state-space model for the drying process is:

$$A = -0.0079365 \quad \text{eq. 6.10}$$

$$B = [-0.015238 \ -0.007619] \quad \text{eq. 6.11}$$

$$C = 0.015625 \quad \text{eq. 6.12}$$

$$D = [0 \ 0] \quad \text{eq. 6.13}$$

For the practical design of a control system, it is desired to control the output rather than the state of the system. Complete state controllability is neither necessary nor sufficient for controlling the output of the system. Considering the system described by equation 6.9 where  $x$  the state vector has a size  $n$ , the control vector  $u$  has a size  $r$ , the output vector  $y$  has a size  $m$ ,  $A$  is a matrix  $n \times n$ ,  $B$  is a matrix  $n \times r$ ,  $C$  is a matrix  $m \times n$  and  $D$  is a matrix  $m \times r$ , it is said to be completely output controllable if and only if it is possible to construct an unconstrained control vector  $u(t)$  that will transfer any given initial output  $y(t_0)$  to any final output  $y(t_1)$  in a finite time interval  $t_0 \leq t \leq t_1$ . Therefore, the system is completely output controllable if and only if the  $m \times (n+1)r$  matrix

$$\left[ \mathbf{CB} \mid \mathbf{CAB} \mid \mathbf{CA}^2\mathbf{B} \mid \dots \mid \mathbf{CA}^{n-1}\mathbf{B} \mid \mathbf{D} \right] \quad \text{eq. 6.14}$$

is of rank  $m$ . In this case the size of the output vector is of 1, the size of the state vector is 1 and the size of the control vector is 2. In other words the matrix of equation 6.14 should

be of rank 1 to be controllable. The matrix of equation 6.14 equivalent to the system that it is being studied is as follows:

$$\text{CON} = [-0.015238 \quad -0.007619 \quad 0.00012094 \quad 6.0469\text{e-}5] \quad \text{eq. 6.15}$$

The rank of this matrix is equal to 1 meaning that the system is controllable.

The system is said to be completely observable if every state  $x(t)$  can be determined from the observation of  $y(t)$  over a finite interval,  $t_0 \leq t \leq t_1$ . The system is, therefore, completely observable if every transition of the state eventually affects every element of the output vector. Mathematically, the system is completely observable if and only if the  $n \times nm$  matrix:

$$\left[ \mathbf{C}^T \mid \mathbf{A}^T \mathbf{C}^T \mid \dots \mid (\mathbf{A}^T)^{n-1} \mathbf{C}^T \right] \quad \text{eq. 6.16}$$

is of rank  $n$  or has  $n$  linearly independent vectors. For the system studied here this matrix is of the form:

$$\text{OBS} = [0.015625 \quad -0.00012401]^T \quad \text{eq. 6.17}$$

which is a matrix of rank 1 making the system completely observable.

Since the system is both observable and controllable then it can be introduced into an MPC algorithm for further studies. MATLAB® provides an MPC toolbox that allows the simulation of linear time invariant models (Bemporad, Morari, and Ricker, 2004-2005; Mathworks, *Qpdantz*). On the other hand the objective function that the toolbox optimizes is different from the one used for the step-response model and drying curve model. The toolbox tries to solve a quadratic programming problem (*Quadratic Programming*) in which the objective function is of the form:

$$\begin{aligned} \mathbf{J} &= \frac{1}{2} \mathbf{x}^T \mathbf{H} \mathbf{x} + \mathbf{c}^T \mathbf{x} & \text{eq. 6.18} \\ \text{subject to : } & \mathbf{A} \mathbf{x} \leq \mathbf{b}; \mathbf{x} \geq \mathbf{x}_{\min} \end{aligned}$$

where  $H$  is a Hessian matrix of a function  $f(x)$ ,  $x \in \mathfrak{R}^n$  and  $c$  is a linear constraint. The purpose of this operation is to minimize the  $x$  vector and solve for the linear system  $Ax = b$ , being the  $x$  vector the input changes and the function needed to develop the Hessian matrix the drying curve model. The results obtained by the MPC toolbox are as follows:

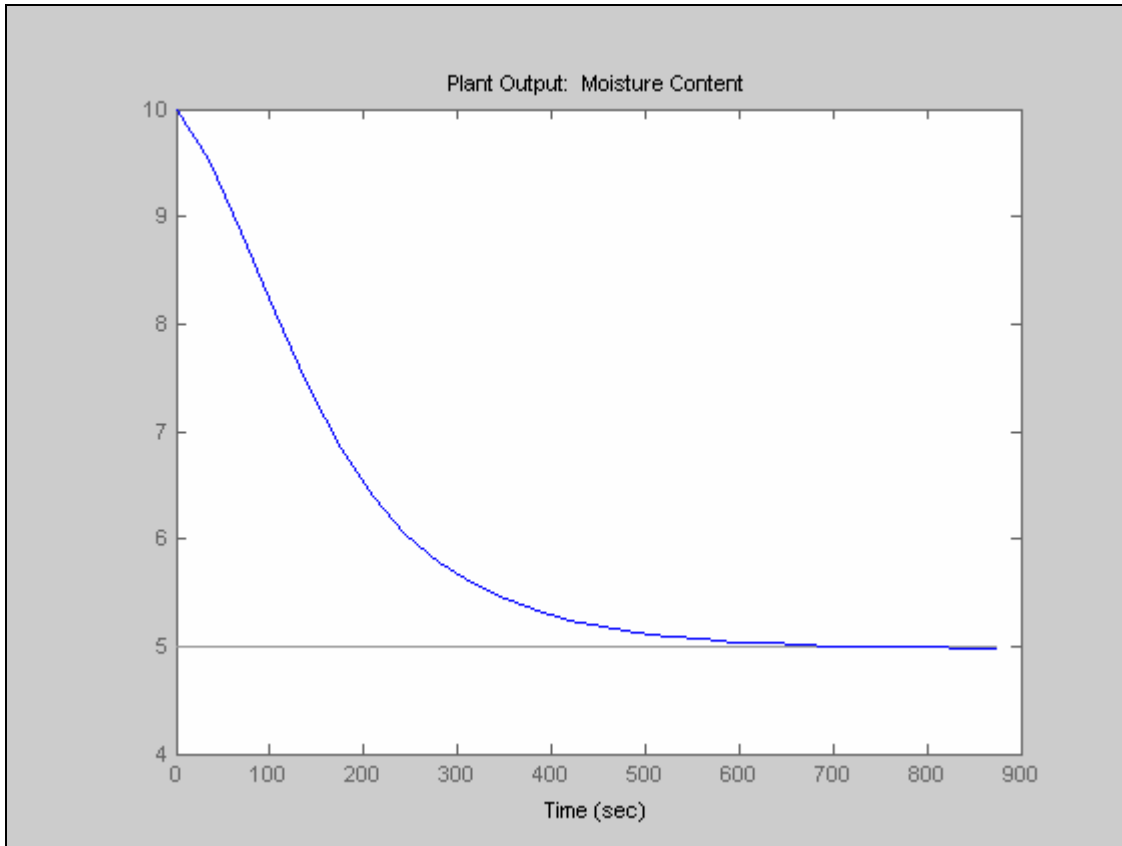


Figure 6.2: Process response of the fluid bed dryer simulated by MPC toolbox in MATLAB®

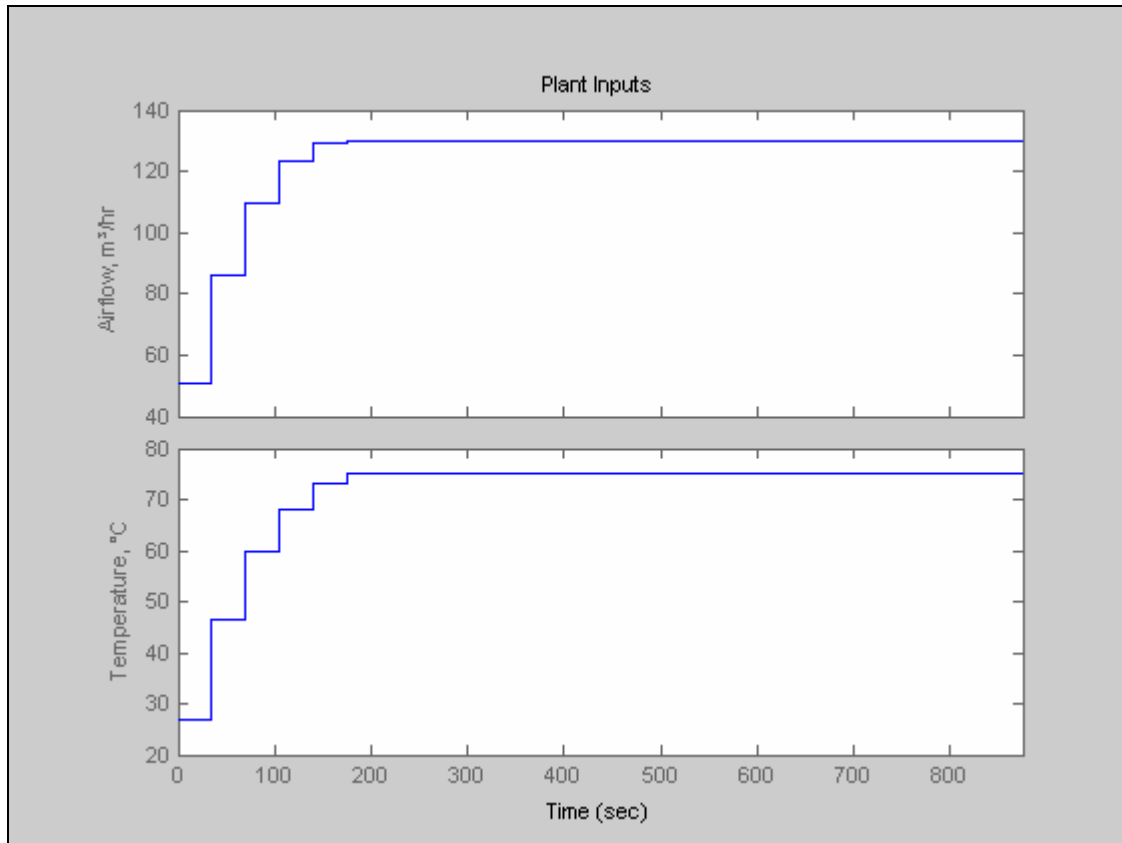


Figure 6.3: Input changes calculated by the MPC toolbox in MATLAB® for the drying process in a fluid bed dryer.

The behavior of the process model simulated by the toolbox represents a more accurate behavior than that simulated by the step-response model. Yet the objective of optimization is not truly achieved, since the fluid bed dryer begins at a low operating conditions and ends the process working the machine at maximum capacity. Normal control behavior would be to start at maximum capacity then start lowering the operational conditions as time passes. But energy consumption is still reduced since the use of maximum capacity is only during the final periods of the drying process rather than during the complete process.

For someone to use a state-space model in an MPC algorithm the operator must use MPC toolboxes, like the one used for this study, since most of MPC controllers does

not adopted state-space theory (Lundh, Molander) If one desires to use a state-space model in a customized MPC algorithm, the model has to be transformed to a time variant model. Even the advantage of toolboxes, like the one provided by MATLAB®, allows you to insert any LTI model, its disadvantage is the lack of customization available to the operator. The operator must work with the optimization priorities that the toolbox is design to solve. In the MATLAB® MPC toolbox® the objective function is design to minimize the input changes having as a weight matrix a Hessian matrix of the process model. The tunings of the controller comes from the linear constraint. On the other hand, the objective function used for the Drying Curve Model MPC and the Step-Response MPC minimizes both input changes and model error, allowing for a better optimization.

## Chapter 7: Development of a PID Controller

### 7.1 PID Design

The most basic strategy for process control is a PID (Proportional-Integral-Derivative) Controller. The purpose of such controller is to reduce the error between the desired step point and the actual point. This does not mean that the trajectory that the PID controller presents is actually the optimal trajectory. Yet if the trajectory presented by the PID controller is optimal, compared to the trajectory calculated by the MPC algorithm, then the MPC algorithm is not required for controlling the fluid bed dryer.

The design of the PID controller is based on the constant-parameter model used in the previous chapter for the state-space and step-response models. For tuning the control parameters Chien and Freuhauf (1990) developed a relationship for PID controllers based on the IMC (Internal Mode Control) method.

The IMC method is based on an assumed process model and leads to analytical expressions for the controller settings. It was first developed by Morari and coworkers during the 1980's. An assumed process model and the controller output are used to calculate the model response. Then the difference between the model response and the process response is used as the input signal for the controller. The advantage of this strategy over PID is when the process contains a large dead time.

In the University of Sherbrooke in Canada Dhib, Thérien, and Broadbent (1999) had implemented an IMC strategy for the drying process of thin textile fabrics using an electric infrared dryer. They compared this method with the behavior obtained from a PI controller. When compared the IMC proved to be a more stable system for closed-loops.

Also the design of the controller did not require the design of compensators for strong interaction between variables.

Chien and Freuhaf, based on this control strategy, developed the following relationships for this model:

$$K_c K = \frac{\tau}{\tau_c} \quad \text{eq. 7.1}$$

$$\tau_1 = \tau \quad \text{eq. 7.2}$$

The parameter  $\tau_c$  is the desired closed-loop time constant. The value of this parameter is presumed ( $\tau_c = \tau = 0.035$ ) obtaining the following tuning results:

**Table 7.1: PI Control parameters**

	<b>Airflow</b>	<b>Temperature</b>
<b><math>K_c</math></b>	-33.33	-66.67
<b><math>\tau_c</math></b>	0.035	0.035

Since the Bode Stability Criterion told us that any  $K_c$  value makes the system stable then the values obtained by the tuning relationship of Chien and Freuhaf are stable parameters.

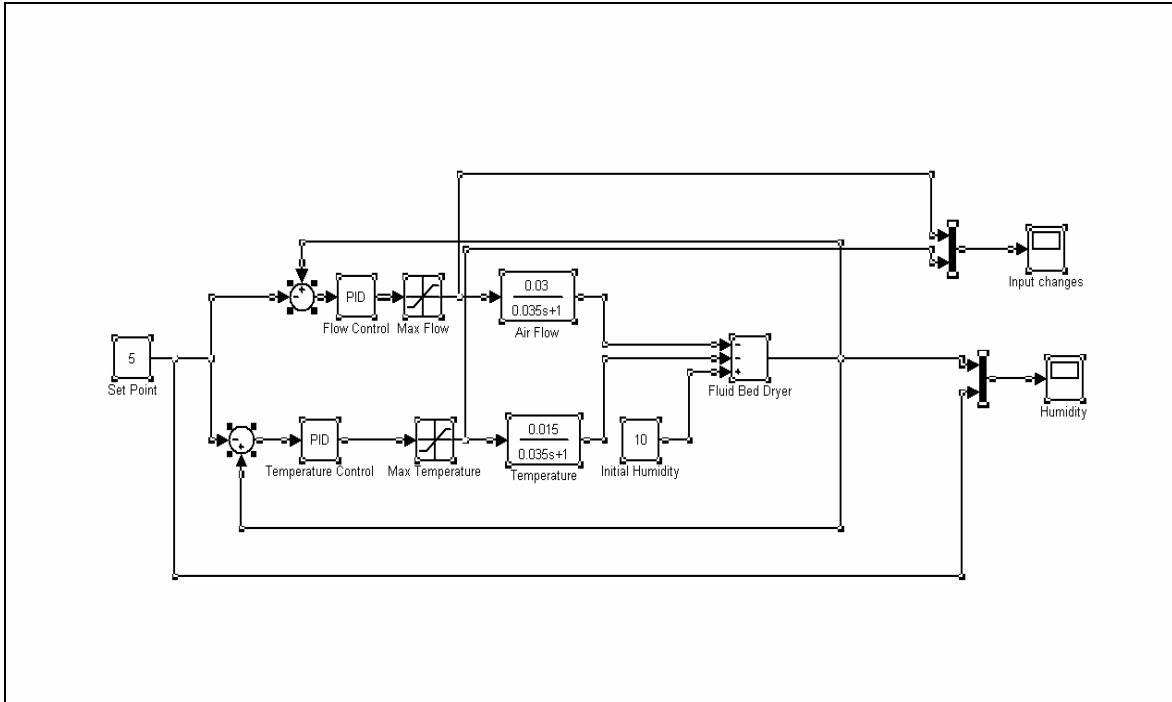


Figure 7.1: Block diagram representation of PID control model for a fluid bed dryer

## 7.2 Simulation Results

In *MatLab*®, *Simulink*® two types of simulations were made to observe the response of the model, one simulation in which the inputs are not bounded by physical restrictions and another in which the inputs are bounded. The following Figures show the response of the model and the input changes made by the unbounded PI controller:



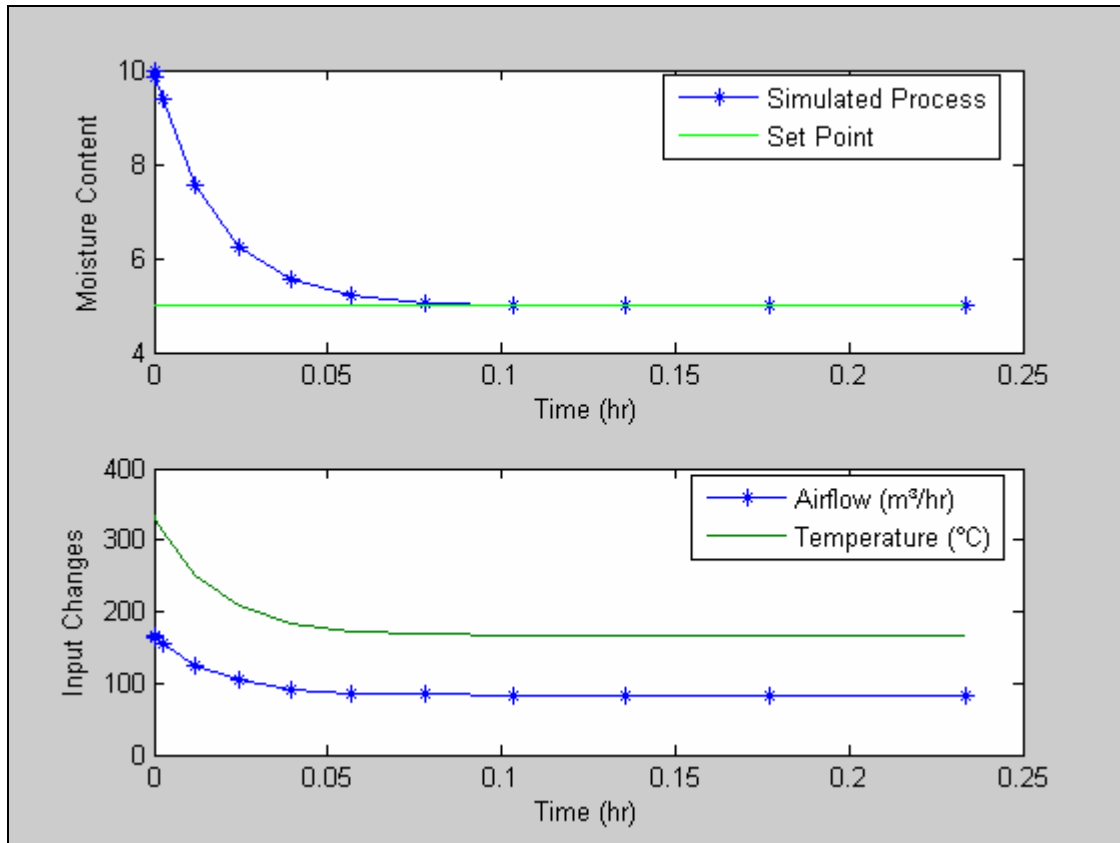


Figure 7.2: Process response and input changes for the fluid bed dryer after PID implementation

It may seem that the PID only requires more tuning to get an equal response like the MPC. But the input changes required to obtain the response seen in Figure 7.1 exceed the physical limitations of the process. The calculations made by the PID give a response not physically possible. The controller calculated that the starting airflow would be around 160 m<sup>3</sup>/hr where the fluid bed dryer can only go as high as 130 m<sup>3</sup>/hr. As for the temperature changes they are extremely high, starting at 330°C and ending around 175°C, while the powder starts to melt at 100°C. But such aggressiveness was expected from a PI control strategy. The main objective of the controller is to reduce the error between the starting point and the set point, not the method used to reduce that error.

For the second simulation, where the physical boundaries were implemented, the system responded as follow:

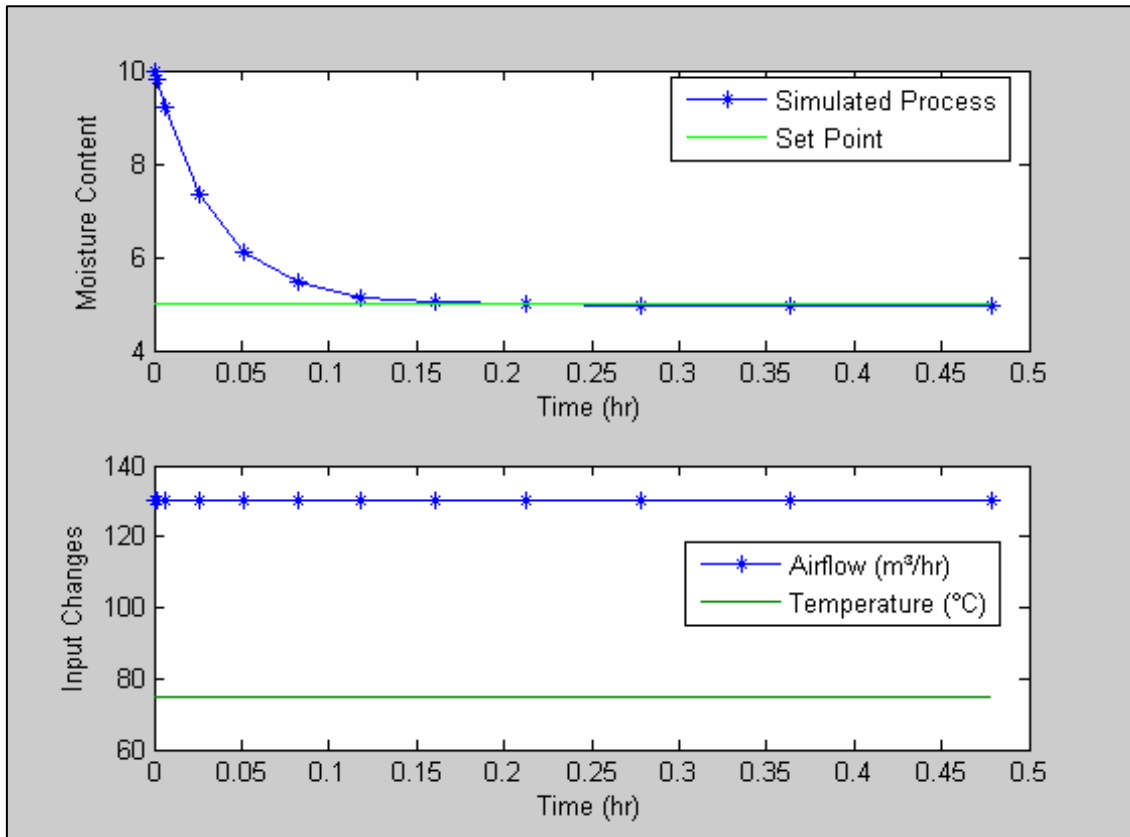


Figure 7.3: Process response and input changes for the fluid bed dryer after physically bounded PID implementation

The behavior of the PI controller is equivalent to an operator monitoring the drying process without any control strategy implemented. Normal monitoring would be to maintain the equipment at maximum capacity and monitor the drying time. This type of monitoring is what the PI controller suggests that should be implemented.

In drying theory there is a point where the humidity of material reaches equilibrium moisture content where, no matter how much you keep drying, it will not go beyond that point. To go beyond this point requires more energy than the one used to dry from the starting humidity up to the equilibrium humidity. If the desired set point was this equilibrium humidity then it would mean that the dryer is consuming more energy than

required. If the case is that the desired set point is not the equilibrium humidity another problem rises.

A PID controller will try to reach the desired set point. If the controller overshoots by the desired set point, in this case humidity, it means that the controller has to let moisture be introduced to the material. For a dryer is not a logical operation to moist a material. This would mean that the controller would be constantly accumulating mathematical error, overloading it and the controller would not respond properly.

Maintaining both input constant and only monitoring drying time, which produces neither energy reduction nor drying time reduction. Compared to the MPC algorithm, where the input changes after a designated interval of time and the drying time is reduced by more than half the normal operation time, the PID algorithm does not provide with any type of optimization for the drying time. Hence the PID control is not a recommended strategy for optimizing the drying process of pharmaceutical powders in a fluid bed dryer, unless some changes are made to the process that makes the PID control behave similar to a MPC control.

## Chapter 8: Conclusions and Recommendations

### 8.1 Conclusions

All of the proposed objectives undertaken in this study were accomplished. The first objective accomplished was the development of a simpler model that describes the drying process. By doing further examination of the drying curve the behavior of the curve is of a certain particularity in which, one may presume that, the functionality of such a curve is exponential.

By the application of fundamental energy and mass balance equations and using mathematical manipulation the drying curve model was developed. To develop the model the following presumptions were made: 1) The drying process is presumed to be continuous process during operating time. 2) The inlet humidity of air is presumed constant since in the industry they work on a controlled environment. 3) The mass transfer area is not constant and does depend on the humidity of the powder. This model is a function of inlet airflow, inlet air temperature and drying time, having adjustable parameters that depend on operational conditions and the material that is being dried. Compared to the first models proposed to describe the drying curve, this model is a more precise lump model. The First Principle Model (FPM) provides a more explicit dependence of airflow compared to the Temperature Drop Model.

Compared to the models presented by Montenegro (2000) and Arocho (2004), the FPM provides a more simplistic model. Different from Montenegro and Arocho's findings, one model is required to describe the complete curve, instead of a different model for a different region in the drying curve. The FPM is a model that requires less adjustable parameters that only depend on operating conditions, not operating conditions

and position in the drying curve. The first principle model results in predictions with  $R^2$  of 0.951908 for a large range of air flow. The effect of particle size on the mass transfer area must be considered. In addition, there is a relationship between the mass transfer area and the moisture content and also between the inter phase air moisture content and the powder moisture content.

The disadvantage that the FPM has over the models proposed by Arocho and Montenegro is that the parameters of the FPM do not have any physical meaning. During the development of the model the adjustable parameters are reduction and combination of physical properties of the material. Having the first principle model a simple structure, as well as the inclusion of operating variables within, makes the model very attractive for control and optimization purposes.

After the First Principle Model was obtained, the MPC algorithm was developed. Since the model is different to the type of models that the literature and commercial toolboxes present a customizable MPC algorithm had to be developed using the same tuning relationships presented by Dougherty and Cooper (2002) for a step-response MPC strategy. The customized MPC algorithm managed to optimize operational conditions (inlet airflow and temperature) and reduce the drying time in the simulation.

This customized MPC was compared to conventional MPC strategies and to PID control strategy. The step-response MPC algorithm lacked any response from the simulated process since the control calculations determined hardly any input change. The step-response model used to determine the predicted trajectory lacked the precision to describe the drying process. Because of the lack of precision the input changes calculated for the process do not provide any response from the process.

The MPC toolbox provided by MATLAB® permits the user to introduce a linear time invariant model as a transfer function, discrete time, or state-space model. The case in which the toolbox was used to simulate the drying process using a state-space model, the toolbox tries to minimize a different type of objective function than the one presented by the literature and used for the customized MPC algorithm and the Step-Response Model MPC algorithm. The minimization of the objective function is the basis for the controller's calculations, so the objective function has to be selected for the specific needs of the operator. The objective function used in the MPC toolbox is focused in obtaining the minimal input changes. The simulation provided by the toolbox did not provide an expected control behavior nor an optimal input change compared to the customized MPC algorithm. Yet compared to the Step-response model, the toolbox provided a better simulation and behavior of the drying process.

When compared to the MPC, the PID provided no optimization of any sort. For the controller to be able to reduce the drying time it required to have the fluid bed dryer working at maximum capacity, which is the same as not having a controller at all and having the equipment work in manual.

## 8.2 Recommendations

The FPM does not describe explicitly the dependence of the model to the physical properties of the material being dried, even though the adjustable parameters do depend directly to the physical properties as to the operational conditions. The behavior of the curve should be used to consider other proposed scientific models. This empirical model should be used as a foundation for the development of more scientific models that could describe the phenomena occurring during the drying process.

## References

1. Alden M., P Torkington, and A.C.R. Strutt, “*Control and instrumentation of a Fluid Bed Dryer using Temperature Difference Technique: I. Development of a working model.*” Powder Technology, 54, pp 15-25. (1988)
2. Arocho, M. Determination of an Empirical Correlation for the Mass Transfer Coefficients of Pharmaceutical Powders in a Fluid Bed Dryer. Thesis M.S. University of Puerto Rico, Mayagüez, PR. (2004)
3. Bakker-Arkema, F.W. and Liu, Q. A Model-Predictive Controller for Grain Drying. Journal of Food Engineering 49: 321-326. (2001)
4. Bemporad, A., Morari, M. and Ricker, N. L. Model Predictive Toolbox for Use with MATLAB. Mathworks, Inc. Natick, MA. (2004-2005).
5. Chandran, A. N., Rao, S. S. and Varma, Y.B.G. Fluidized Bed Drying of Solids. AIChE Journal Vol. 36 No. 1. (1990).
6. Chien, I.L. and Fruehauf, P.S. Consider IMC Tuning to Improve Controller Performance. Chemical Engineering Progress, 86 (10), 33, (1990).
7. Cutler, R. C., and Ramaker, B. L. Dynamic Matrix Control-A Computer Control Algorithm. Proc. Joint Auto Control Conf., Paper WP5-B, San Francisco. (1980)
8. Dhib, R., Thérien, N. and Broadbent, A. Model-Based Multivariable Control of the Drying of a Thin Sheet of Fibres in a Continuous Infrared Dryer. Canadian Journal of Chemical Engineering 77: 1055, (1999).
9. Dougherty, D. and Cooper, D. 2003 A Practical Multiple Model Adaptive Strategy for Multivariable Model Predictive Control. Control Engineering Practice, 11: 649-664.
10. Edgar, T., Mellichamp, D. and Seborg, D. 2004. Process Dynamics and Control: 2<sup>nd</sup> edition. John Wiley & Sons, Inc., USA. 534-551.
11. Fiske, T., Ghosh, A. 2003. Apply Model Predictive Control to Reduce Batch Cycle Time and Increase Consistency.  
<http://www.easydeltav.com/news/viewpoint/ARC.pdf>
12. Lipták B., “*Optimizing Dryer Performance Through Better Control.*” Chem. Eng. Prog., February, pp. 110-114, (1998).
13. Lundh, M. and Molander, State-space Models in Model Predictive Control. ABB Automation Products AB.

14. Mathworks. Qpdantz.  
<http://www.mathworks.com/access/helpdesk/help/toolbox/mpc/qpdantz.html>
15. Montenegro J., Modeling and Automation of a Fluid Bed Dryer for Determination of Optimum Drying End Points of Pharmaceutical Granulations. M.Sc. Thesis, (2000).
16. Montgomery D.C. Design and analysis of experiments, J. Wiley & Sons, New York, U.S., Five ed., pp 573-583, (1996).
17. Morris, C. E. Food Engineers Apply Predictive Control. Food Engineering Dec. 53-56. (1998)
18. Quadratic Programming.  
<http://www-fp.mcs.anl.gov/otc/Guide/OptWeb/continuous/constrained/qprog/>
19. Richalet, J. *et al.* Model Predictive Heuristic Control: Applications to Industrial Processes. Automatica, 14, 413, (1978).
20. Robinson J.W. Improve dryer control. Chem.Eng. Prog., pp. 28-33, (1992).
21. Shinskey F.G., "*Process Control Systems.*" McGraw Hill Chem. Eng. Series, Second ed., New York, US, pp 322-325, (1979).
22. Treybal R.E., "*Mass Transfer Operations.*" McGraw Hill Chem. Eng. Series, pp 63, 576-599, (1978).
23. Valencia, A. F. Modeling and Control of Continuous Tumble Mixing of Granular Materials. Thesis M.S. University of Puerto Rico, Mayagüez, P.R., (2005).
24. Wang Z.H. and G. Chen, "*Heat and mass transfer in batch fluidized-bed of porous particles.*" Chem. Eng. Sc., 55, pp. 1857-1869, (2000).
25. Wildfong, P.L.D., *et al.* "Accelerated Fluid Bed Drying Using NIR Monitoring and Phenomenological Modeling: Method Assessment and Formulation Suitability" *Journal of Pharmaceutical Science* Vol. 91, No. 3 (2002).



## Appendix A. Parameter Definition for the First Principle Model

### A. Air balance:

$$\Gamma_{o,m}(s) = \frac{K_{m2,1}}{\tau_{m2}s + 1} Q_{air,i}(s) + \frac{K_{m2,2}}{\tau_{m2}s + 1} \Gamma_i(s) - \frac{K_{m2,3}}{\tau_{m2}s + 1} Q_{air,o}(s)$$

$$\tau_{m2} = \frac{V}{q_{airout,steady-state}}$$

$$K_{m2,1} = \frac{\rho_{airin,steady-state}}{q_{airout,steady-state} C_{T_{pout}}}$$

$$K_{m2,2} = \frac{q_{airin,steady-state} C_{T_{pin}}}{q_{airout,steady-state} C_{T_{pout}}}$$

$$K_{m2,3} = \frac{\rho_{airout,steady-state}}{q_{airout,steady-state} C_{T_{pout}}}$$

$C_{T_p}$  = Steady state parameters for air density function

### B. Energy balance around air:

$$\Gamma_{o,E}(s) = \frac{K_{E1,1}}{\tau_{E1}s + 1} Q_{air,i}(s) + \frac{K_{E1,2}}{\tau_{E1}s + 1} \Gamma_i(s) - \frac{K_{E1,3}}{\tau_{E1}s + 1} Q_{air,o}(s) - \frac{K_{E1,4}(\tau_{1E1}s + 1)}{\tau_{E1}s + 1} \hat{Y}_{air,o}(s)$$

$$\tau_{E1} = \frac{V \left[ T_{out} C_{p_{out}} C_{T_{pout}} + \rho_{airout,steady-state} C_{T_{pout}} + \rho_{airout,steady-state} T_{out} C_{T_{pout}} \right]}{q_{airout,steady-state} C_{p_{out}} T_{out} C_{T_{pout}} + q_{airout,steady-state} \rho_{airout,steady-state} T_{out} C_{T_{pout}} + q_{airout,steady-state} \rho_{airout,steady-state} C_{p_{out}}}$$

$$\tau_{1E1} = \frac{V \rho_{airout,steady-state} T_{out} C_{T_{pout}}}{q_{airout,steady-state} \rho_{airout,steady-state} T_{out} C_{y_{out}}}$$

$$K_{E1,1} = \frac{\rho_{airin,steady-state} T_{in} C_{pin}}{q_{airout,steady-state} C_{p_{out}} T_{out} C_{T_{pout}} + q_{airout,steady-state} \rho_{airout,steady-state} T_{out} C_{T_{pout}} + q_{airout,steady-state} \rho_{airout,steady-state} C_{p_{out}}}$$

$$K_{E1,2} = \frac{q_{airin,steady-state} C_{pin} T_{in} C_{T_{pin}} + q_{airin,steady-state} \rho_{airin,steady-state} T_{in} C_{T_{pin}} + q_{airin,steady-state} \rho_{airin,steady-state} C_{pin}}{q_{airout,steady-state} C_{p_{out}} T_{out} C_{T_{pout}} + q_{airout,steady-state} \rho_{airout,steady-state} T_{out} C_{T_{pout}} + q_{airout,steady-state} \rho_{airout,steady-state} C_{p_{out}}}$$

$$K_{E1,3} = \frac{\rho_{airout,steady-state} T_{out} C_{p_{out}}}{q_{airout,steady-state} C_{p_{out}} T_{out} C_{T_{pout}} + q_{airout,steady-state} \rho_{airout,steady-state} T_{out} C_{T_{pout}} + q_{airout,steady-state} \rho_{airout,steady-state} C_{p_{out}}}$$

$$K_{E1,4} = \frac{q_{airout,steady-state} \rho_{airout,steady-state} T_{out} C_{y_{out}}}{q_{airout,steady-state} C_{p_{out}} T_{out} C_{T_{pout}} + q_{airout,steady-state} \rho_{airout,steady-state} T_{out} C_{T_{pout}} + q_{airout,steady-state} \rho_{airout,steady-state} C_{p_{out}}}$$

$C_{y_{out}}$  = Steady state parameters for the heat transfer coefficient

### C. Output Airflow:

$$Q_{\text{air,o}}(s) = \frac{K_{q1}(\tau_{lq0,1}s+1)}{\tau_{q0}s+1} Q_{\text{air,i}}(s) + \frac{K_{q2}(\tau_{lq0,2}s+1)}{\tau_{q0}s+1} \Gamma_i(s) - \frac{K_{q3}(\tau_{lq0,3}s+1)(\tau_{1_{E1}}s+1)}{\tau_{q0}s+1} \hat{Y}_{\text{air,o}}(s)$$

$$\tau_{q0} = \frac{K_{E1,3}\tau_{m2} - K_{m2,3}\tau_{E1}}{K_{E1,3} - K_{m2,3}}$$

$$\tau_{lq0,1} = \frac{K_{E1,1}\tau_{m2} - K_{m2,1}\tau_{E1}}{K_{E1,3} - K_{m2,3}}$$

$$\tau_{lq0,2} = \frac{K_{E1,2}\tau_{m2} - K_{m2,2}\tau_{E1}}{K_{E1,3} - K_{m2,3}}$$

$$\tau_{lq0,3} = \frac{K_{E1,4}\tau_{m2}}{K_{E1,3} - K_{m2,3}}$$

$$K_{q1} = \frac{K_{E1,1} - K_{m2,1}}{K_{E1,3} - K_{m2,3}}$$

$$K_{q2} = \frac{K_{E1,2} - K_{m2,2}}{K_{E1,3} - K_{m2,3}}$$

$$K_{q3} = \frac{K_{E1,4}}{K_{E1,3} - K_{m2,3}}$$

### D. Output Temperature:

$$\Gamma_o(s) = \frac{K_{T1}(\tau_{IT1}s+1)}{(\tau_{q0}s+1)(\tau_{m2}s+1)} Q_{\text{air,i}}(s) + \frac{K_{T2}(\tau_{IT2}s+1)}{(\tau_{q0}s+1)(\tau_{m2}s+1)} \Gamma_i(s) - \frac{K_{T3}(\tau_{lq0,3}s+1)(\tau_{1_{E1}}s+1)}{(\tau_{q0}s+1)(\tau_{m2}s+1)} \hat{Y}_{\text{air,o}}(s)$$

$$\tau_{IT1} = \frac{K_{m2,1}\tau_{q0} - K_{m2,3}K_{q1}\tau_{lq0,1}}{K_{m2,1} - K_{m2,3}K_{q1}}$$

$$\tau_{IT2} = \frac{K_{m2,2}\tau_{q0} - K_{m2,3}K_{q2}\tau_{lq0,1}}{K_{m2,2} - K_{m2,3}K_{q2}}$$

$$K_{T1} = K_{m2,1} - K_{m2,3}K_{q1}$$

$$K_{T2} = K_{m2,2} - K_{m2,3}K_{q2}$$

$$K_{T3} = K_{m2,3}K_{q3}$$

### E. Saturation Temperature:

$$\Gamma_s(s) = \frac{K_{E2,1}(\tau_{IE2,1}s+1)(\tau_{IE2,2}s+1)}{(\tau_{q0}s+1)(\tau_{m2}s+1)(\tau_{E2}s+1)} Q_{\text{air,i}}(s) + \frac{K_{E2,1}(\tau_{IE2,3}s+1)(\tau_{IE2,4}s+1)}{(\tau_{q0}s+1)(\tau_{m2}s+1)(\tau_{E2}s+1)} \Gamma_i(s) + \frac{K_{E2,3}(\tau_{lq0,3}s+1)(\tau_{IE1}s+1)}{(\tau_{q0}s+1)(\tau_{m2}s+1)(\tau_{E2}s+1)} \hat{Y}_{\text{air,o}}(s)$$

$$\tau_{E2} = \frac{m_{\text{pow}} C_{p \text{ pow}}}{U_{\text{steady-state}} A}$$

$K_{E2,1}(\tau_{IE2,1}s+1)(\tau_{IE2,2}s+1)$  is obtained through the factorization of the following equation :  
 $UAK_{T1}(\tau_{IT1}s+1) + [AT_{\text{out}}C_{q_h} - AT_sC_{q_h}](\tau_{q0}s+1)(\tau_{m2}s+1)$

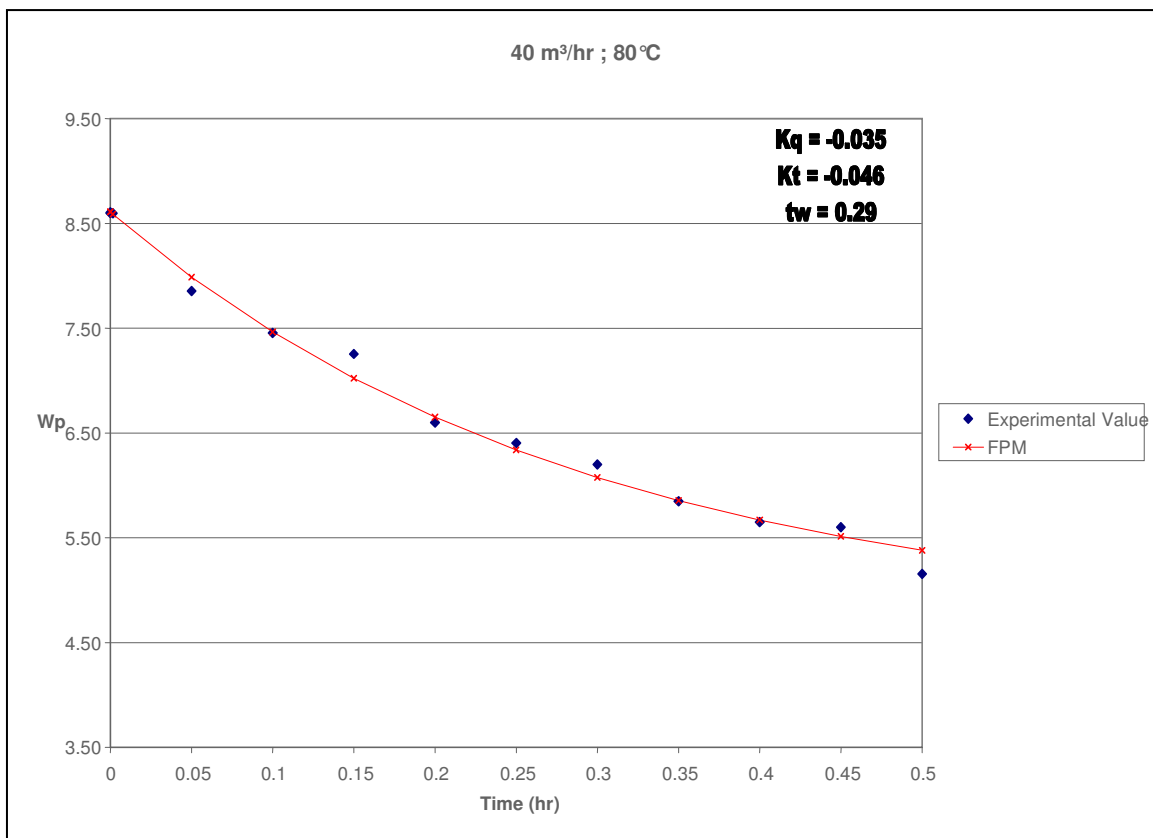
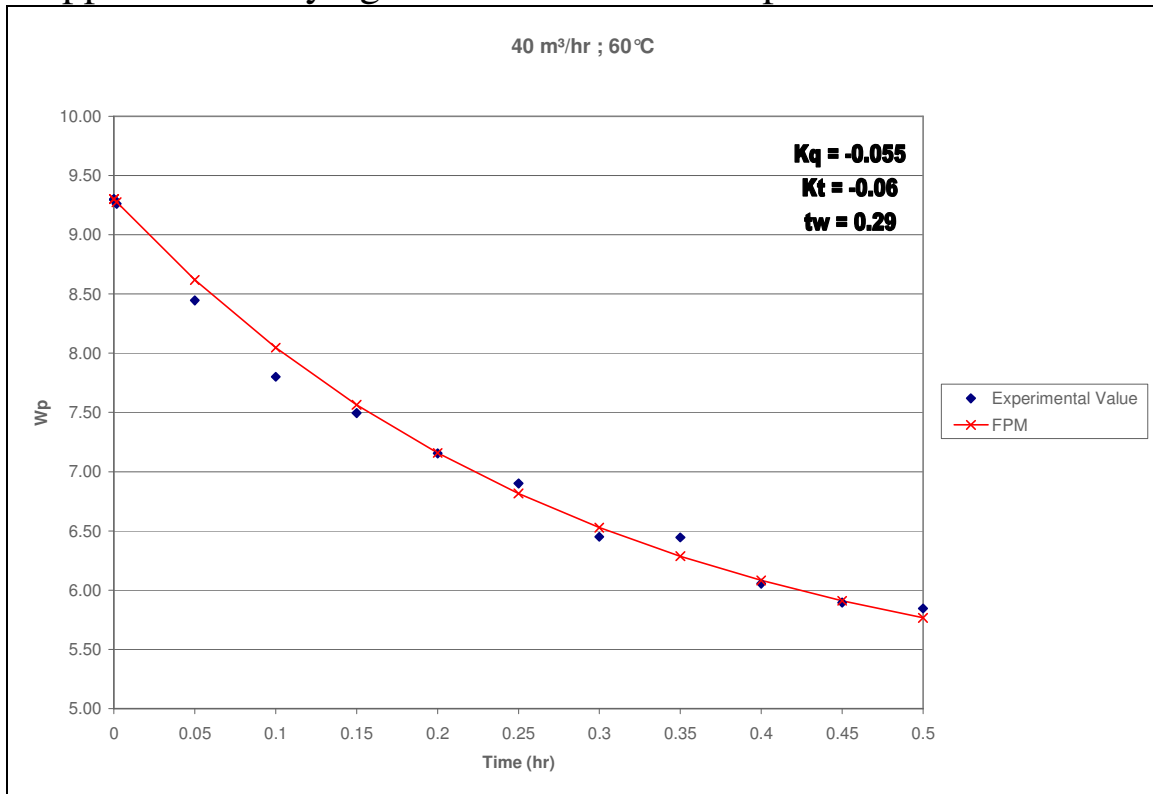
$K_{E2,1}(\tau_{IE2,3}s+1)(\tau_{IE2,4}s+1)$  is obtained through the factorization of the following equation :  
 $UAK_{T2}(\tau_{IT2}s+1) + [AT_{\text{out}}C_{T_h} - AT_sC_{T_h}](\tau_{q0}s+1)(\tau_{m2}s+1)$

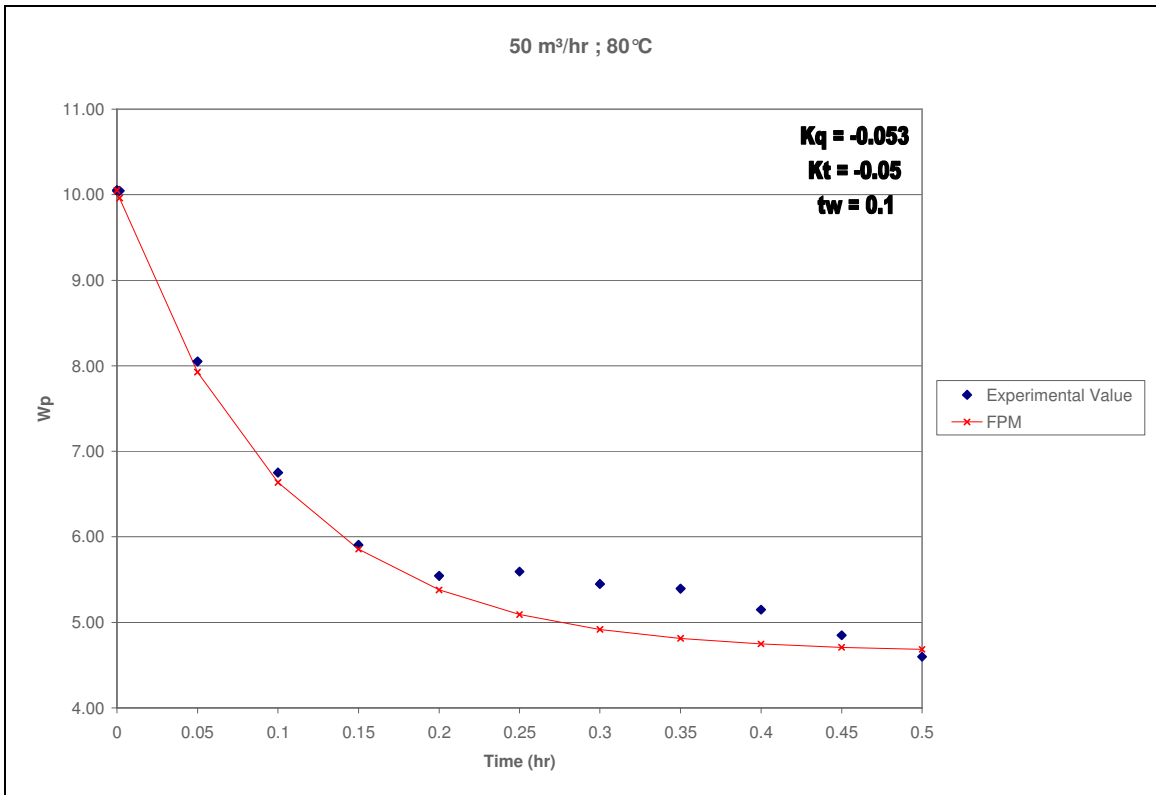
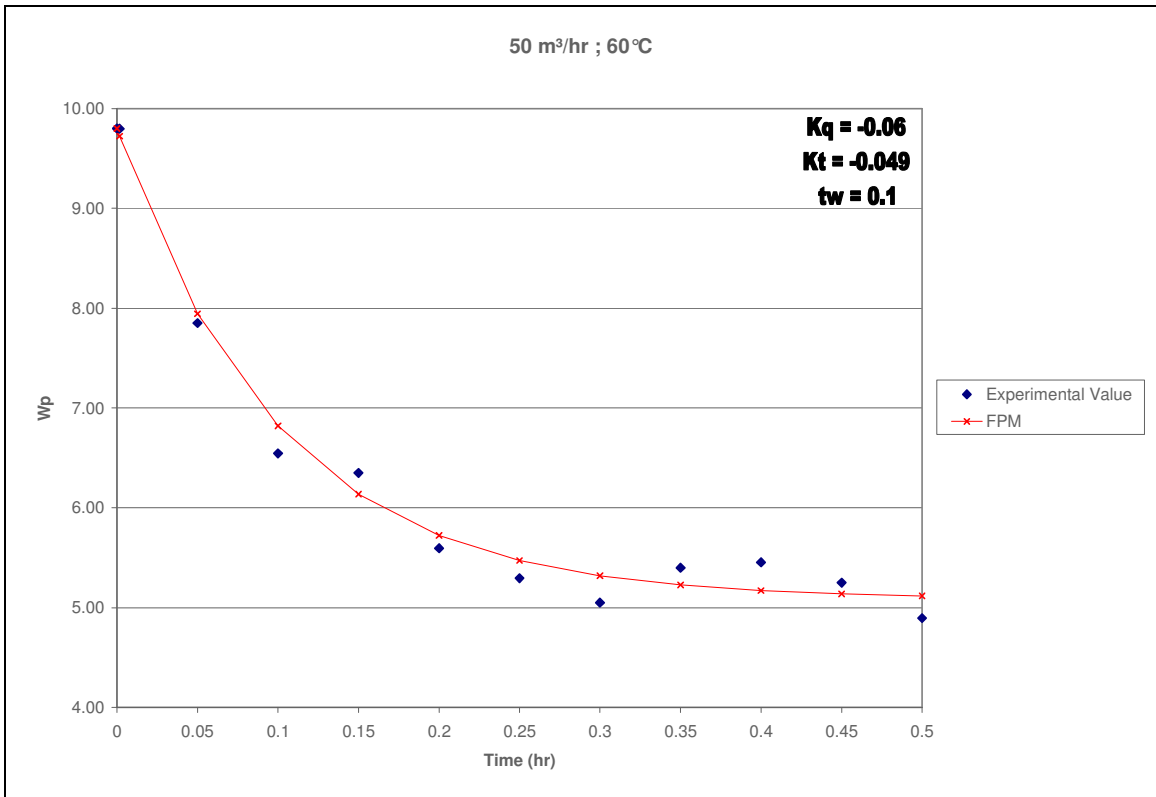
$$K_{E2,3} = UAK_{T3}$$

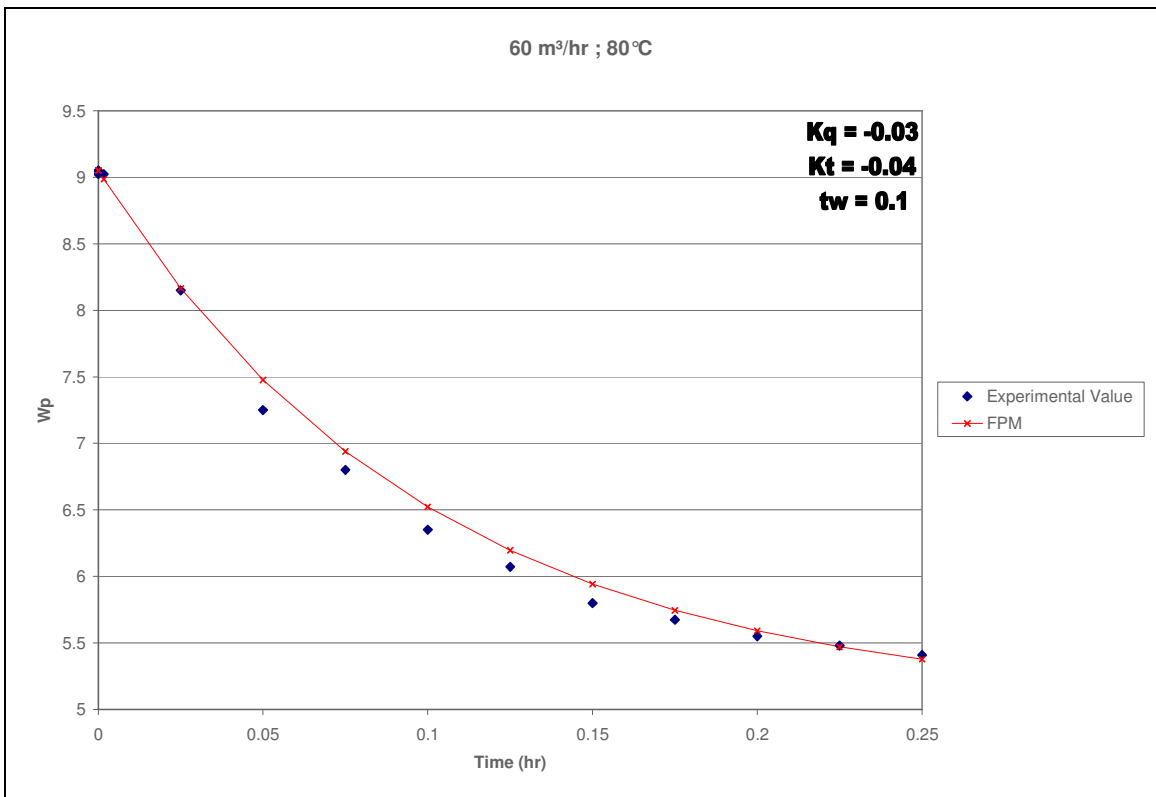
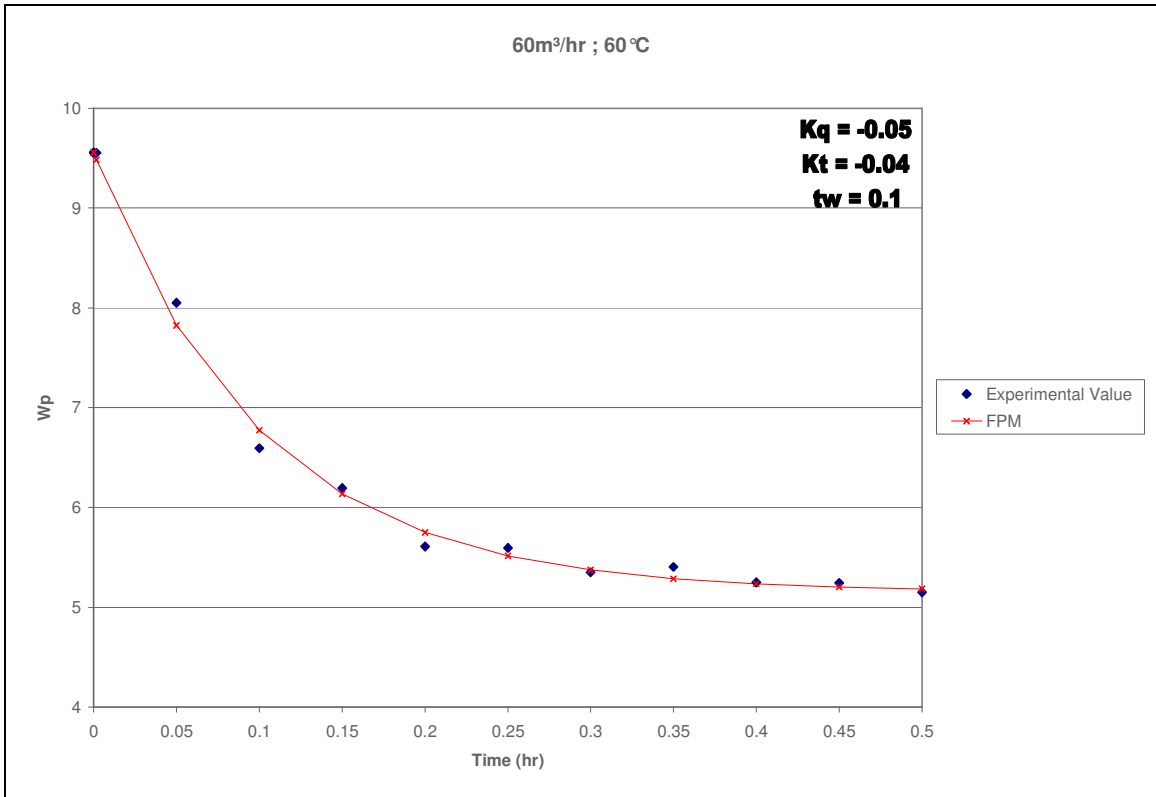
$C_{T_h}$  = Steady state parameter for overall heat transfer coefficient with respect to temperature

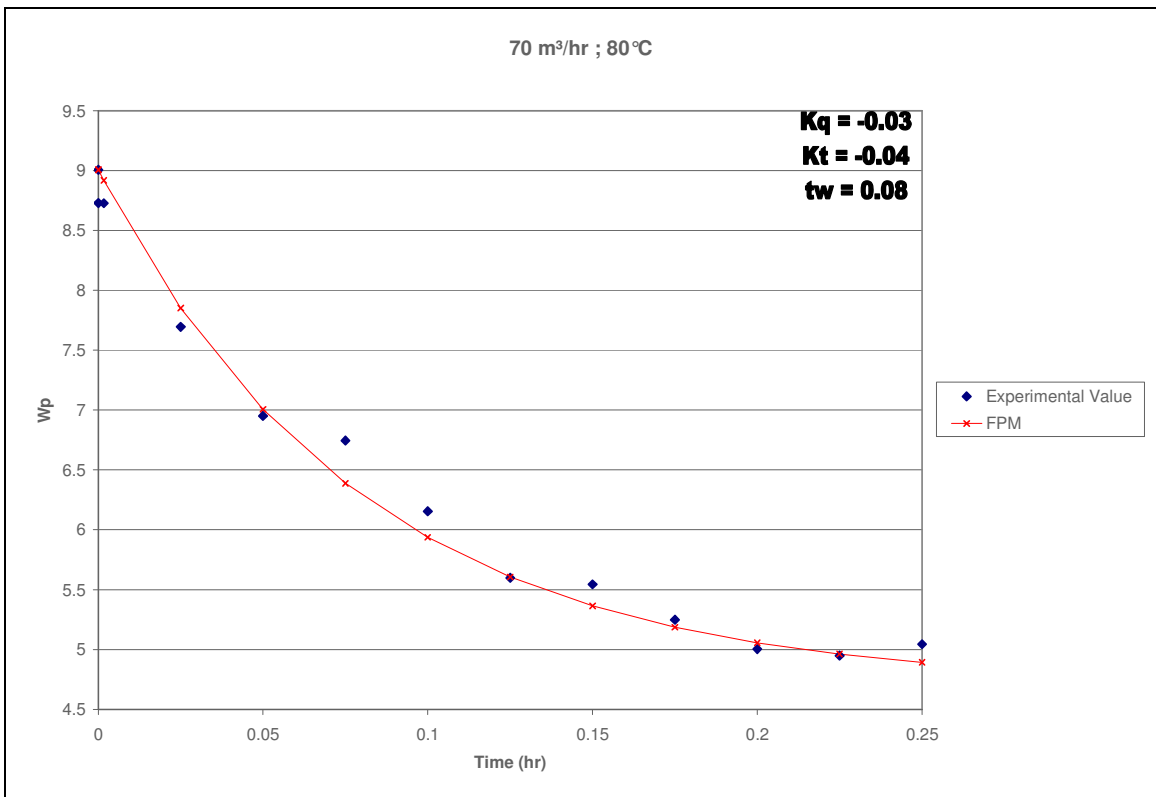
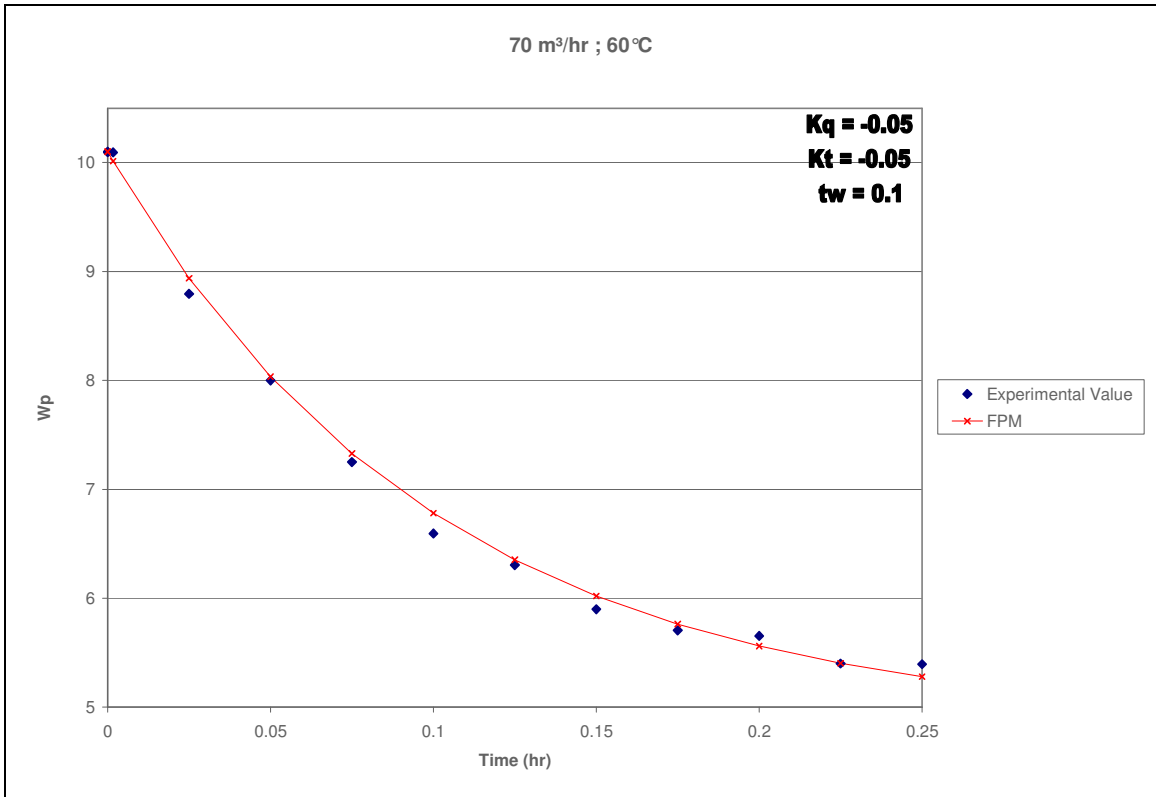
$C_{q_h}$  = Steady state parameter for overall heat transfer coefficient with respect to airflow

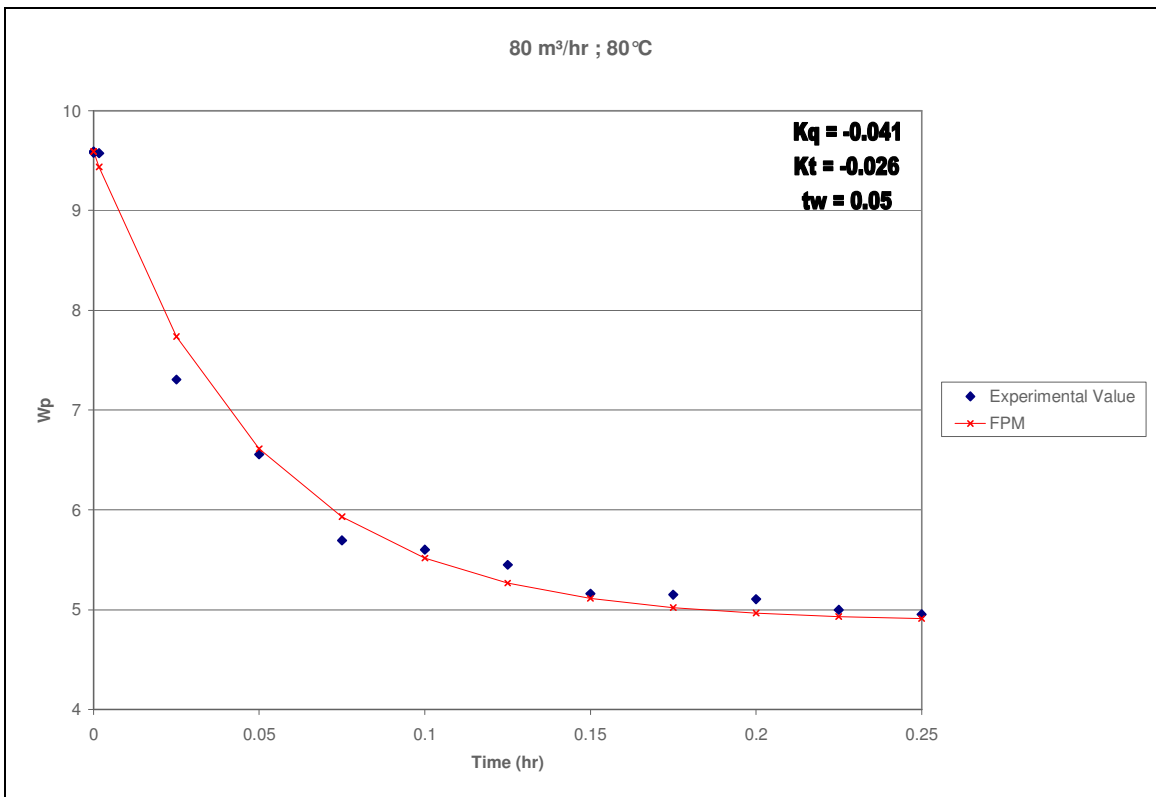
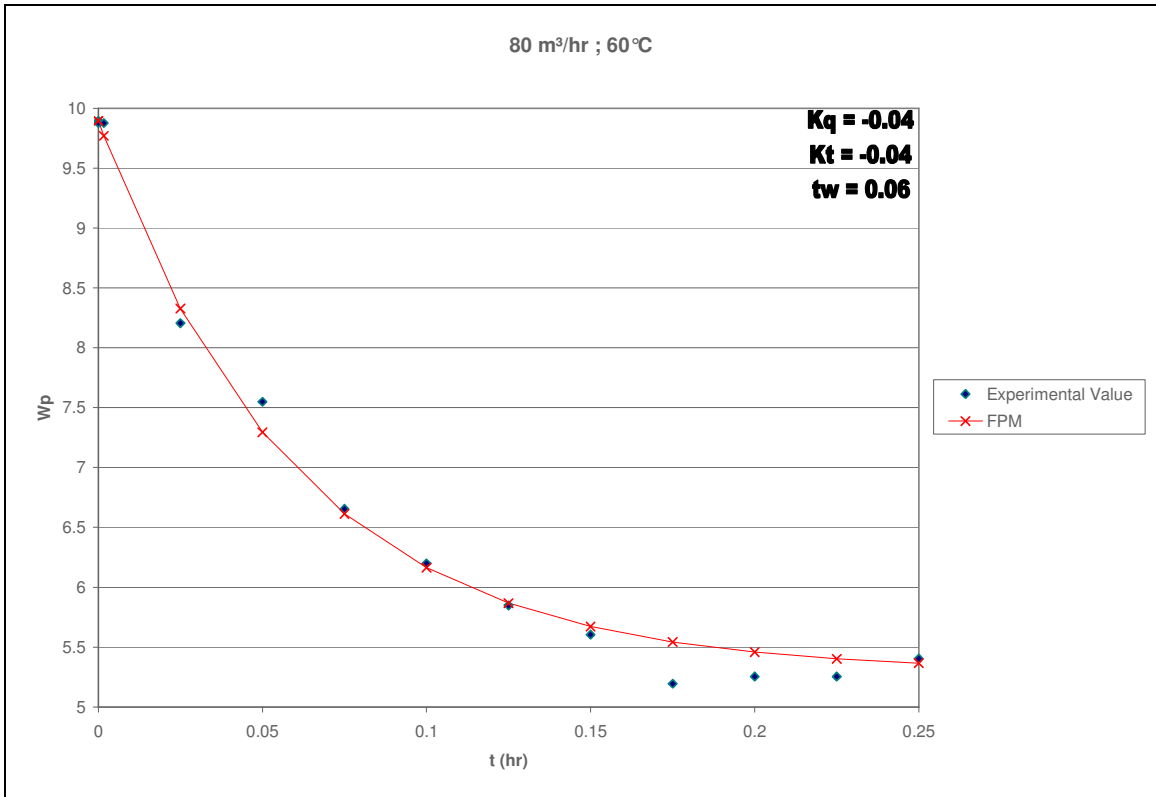
## Appendix B. Drying Curves at Different Operational Conditions













## Appendix C. Model Predictive Control Algorithms

### A. FPM Model Predictive Control Algorithm:

#### A.1: MATLAB® Algorithm

```
clear;
initialHumidity = 10;
setPoint = 5;
%Control Parameters
Kq = -0.05;
Kt = -0.04;
tau = 0.1;
P=51;
M=22;
tiempo = 0;
h=1;
for k=1:1:P
    if h<M-1
        K(k,h)=Kq*(1-exp(-tiempo/tau));
        K(k,h+1)=Kt*(1-exp(-tiempo/tau));
    else
        K(k,21)=Kq*(1-exp(-tiempo/tau));
        K(k,22)=Kt*(1-exp(-tiempo/tau));
    end
    h=h+2;
    tiempo=tiempo+(0.5/P);
end

Q=0.3*eye(P);
for k=1:M
    if k<=M/2
        R(k,k)=0.06092;
    else
        R(k,k)=0.02879;
    end
end

R=0.0004*R;
Kc = (inv((K'*Q*K)+R))*K'*Q;

%Initial values
n = size(K);
yReferenceTrajectory = setPoint*ones(n(1,1),1);
yPredictedTrajectory = initialHumidity*ones(n(1,1),1);
error = 0;
yOutput = initialHumidity;
loopCount = 1;

for t=0:0.5/n(1,1):0.5

    %Control Law%
```

```

ErrorReferencePredicted = yReferenceTrajectory - yPredictedTrajectory -
(error*ones(n(1,1),1));
deltaU = Kc*ErrorReferencePredicted;
%Physical Restrictions%
for i=1:2:22
    %air flow
    if deltaU(i)>130
        deltaU(i) = 130;
    elseif deltaU(i)<-130
        deltaU(i) = -130;
    end
    %air temperature
    if deltaU(i+1)>75
        deltaU(i+1) = 75;
    elseif deltaU(i+1)<-100
        deltaU(i+1) = -100;
    end
end

CurrentQ(loopCount)=deltaU(3);
CurrentT(loopCount)=deltaU(4);
Humidity(loopCount)=initialHumidity;

if loopCount >1
    if CurrentQ(loopCount)==CurrentQ(loopCount-1) &&
CurrentT(loopCount)==CurrentT(loopCount-1)
        initialHumidity = Humidity(loopCount);
    else
        initialHumidity = yOutput;
    end
end

%Real Process Simulation%
% Seleccion de modelo
if deltaU(3)==0 && deltaU(4)==0
    if loopCount > 1
        Wp(loopCount)=Wp(loopCount-1);
    else
        kFlujo = -0.044;
        kTemperatura = -0.055;
        tau = 0.29;
    end

elseif deltaU(3)==0 && deltaU(4)>0
    kFlujo = -0.044;
    kTemperatura = -0.055;
    tau = 0.29;

elseif deltaU(3)>0 && deltaU(3)<=10
    if deltaU(4)>=0 && deltaU(4)<=100
        kFlujo = -0.044;
        kTemperatura = -0.055;
        tau = 0.29;
    end

elseif deltaU(3)>=11 && deltaU(3)<=40
    if deltaU(4)>=0 && deltaU(4)<=35

```

```

        kFlujo = -0.055;
        kTemperatura = -0.06;
        tau = 0.29;
    elseif deltaU(4)>=36 && deltaU(4)<=100
        kFlujo = -0.035;
        kTemperatura = -0.046;
        tau = 0.29;
    end

elseif deltaU(3)>=41 && deltaU(3)<=50
    if deltaU(4)>=0 && deltaU(4)<=35
        kFlujo = -0.06;
        kTemperatura = -0.049;
        tau = 0.1;
    elseif deltaU(4)>=36 && deltaU(4)<=100
        kFlujo = -0.053;
        kTemperatura = -0.05;
        tau = 0.1;
    end

elseif deltaU(3)>=51 && deltaU(3)<=60
    if deltaU(4)>=0 && deltaU(4)<=35
        kFlujo = -0.05;
        kTemperatura = -0.04;
        tau = 0.1;
    elseif deltaU(4)>=36 && deltaU(4)<=100
        kFlujo = -0.03;
        kTemperatura = -0.04;
        tau = 0.1;
    end

elseif deltaU(3)>=61 && deltaU(3)<=70
    if deltaU(4)>=0 && deltaU(4)<=35
        kFlujo = -0.05;
        kTemperatura = -0.05;
        tau = 0.1;
    elseif deltaU(4)>=36 && deltaU(4)<=100
        kFlujo = -0.03;
        kTemperatura = -0.04;
        tau = 0.08;
    end

elseif deltaU(3)>=71 && deltaU(3)<=80
    if deltaU(4)>=0 && deltaU(4)<=35
        kFlujo = -0.04;
        kTemperatura = -0.04;
        tau = 0.06;
    elseif deltaU(4)>=36 && deltaU(4)<=100
        kFlujo = -0.041;
        kTemperatura = -0.026;
        tau = 0.05;
    end
end

```

```

elseif deltaU(3)>=81 && deltaU(3)<=130
    if deltaU(4)>=0 && deltaU(4)<=100
        kFlujo = -0.041;
        kTemperatura = -0.033;
        tau = 0.05;
    end

end

GF(loopCount) = kFlujo;
GT(loopCount) = kTemperatura;
Ttau(loopCount) = tau;

yOutput = ((kFlujo*deltaU(3))+(kTemperatura*deltaU(4)))*(1-exp(-t/tau))
+ initialHumidity;
ySim = ((-0.03*deltaU(3))+(-0.015*deltaU(4)))*(1-exp(-t/0.035)) +
initialHumidity;

Wp(loopCount) = yOutput;
yModelo(loopCount) = ySim;

Time(loopCount) = t;

if Wp(loopCount)<=setPoint
    break
end

error = Wp(loopCount) - yModelo(loopCount);

time = t;
h=1;
for k=1:1:51
    time=time+(0.5/51);
    if h<M-1
        G(k,h)=-0.03*(1-exp(-time/0.035));
        G(k,h+1)=-0.015*(1-exp(-time/0.035));
    else
        G(k,21)=-0.03*(1-exp(-time/0.035));
        G(k,22)=-0.015*(1-exp(-time/0.035));
    end
    h=h+2;
end

yPredictedTrajectory = G*deltaU + initialHumidity*ones(n(1,1),1);

loopCount = loopCount + 1;

end
% Grafica de resultados
% loopCount = loopCount - 2;
Y = [tf(-0.03,[126 1]) tf(-0.015,[126 1])];
[A,B,C,D] = ssdata(Y);
Yss = ss(A,B,C,D);
Con = [B A*B];
Obs = [C;C*A];
control = rank(Con);

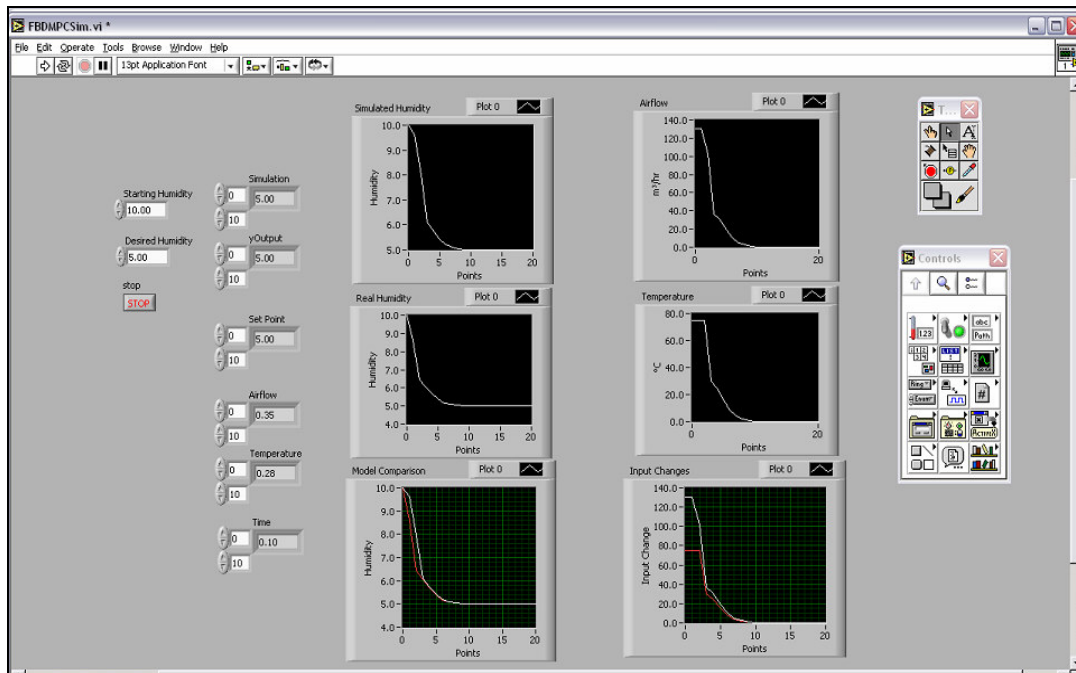
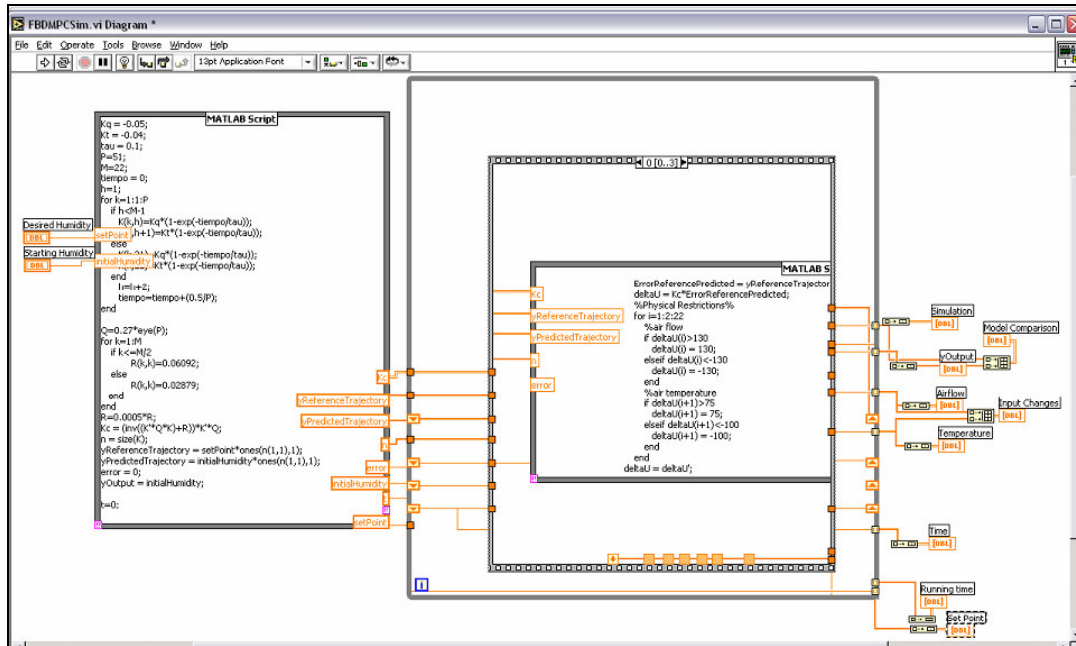
```

```

observation = rank(Obs);
figure (1);
subplot(2,1,1); plot(Time(1:loopCount), Wp(1:loopCount), '-
*', Time(1:loopCount), yModelo(1:loopCount), '--
', Time(1:loopCount), yReferenceTrajectory(1:loopCount), 'g');
subplot(2,1,2); plot(Time(1:loopCount), CurrentQ(1:loopCount), '-
*', Time(1:loopCount), CurrentT(1:loopCount));
figure(2);
bode (Y);

```

## A.2 LabView® Algorithm



## B. Step-Response Model Predictive Control Algorithm

```
initialHumidity = 10;
setPoint = 5;
P=51;
V=22;
Q=eye(P);
for k=1:V
    if k<=V/2
        R(k,k)=0.06092;
    else
        R(k,k)=0.02879;
    end
end
R=R;
Kc = (inv((Sb1'*Q*Sb1)+R))*Sb1'*Q;
n = size(Sb1);
yReferenceTrajectory = setPoint*ones(n(1,1),1);
yPredictedTrajectory = initialHumidity*ones(n(1,1),1);
error = 0;
yOutput = initialHumidity;
loopCount = 1;
counter = 1;

for t=0:0.5/n(1,1):0.4902

    %Control Law%
    ErrorReferencePredicted = yReferenceTrajectory - yPredictedTrajectory;
    deltaU = Kc*ErrorReferencePredicted;
    %Physical Restrictions%
    for i=1:2:22
        if deltaU(i)>130
            deltaU(i) = 130;
        elseif deltaU(i)<-130
            deltaU(i) = -130;
        end
        if deltaU(i+1)>75
            deltaU(i+1) = 75;
        elseif deltaU(i+1)<-75
            deltaU(i+1) = -75;
        end
    end
    end

    CurrentQ(loopCount)=deltaU(1);
    CurrentT(loopCount)=deltaU(2);
    Humidity(loopCount)=initialHumidity;

    if loopCount >1
        if CurrentQ(loopCount)==CurrentQ(loopCount-1) &&
CurrentT(loopCount)==CurrentT(loopCount-1)
            initialHumidity = Humidity(loopCount);
        else
            initialHumidity = yOutput;
        end
    end
end
```

```

%Real Process Simulation%
if deltaU(1)==0 && deltaU(2)==0
    kFlujo = -0.044;
    kTemperatura = -0.055;
    tau = 0.29;

elseif deltaU(1)==0 && deltaU(2)>0
    kFlujo = -0.044;
    kTemperatura = -0.055;
    tau = 0.29;

elseif deltaU(1)>0 && deltaU(1)<=10
    if deltaU(2)>=0 && deltaU(2)<=100
        kFlujo = -0.044;
        kTemperatura = -0.055;
        tau = 0.29;
    end

elseif deltaU(1)>=11 && deltaU(1)<=40
    if deltaU(2)>=0 && deltaU(2)<=35
        kFlujo = -0.055;
        kTemperatura = -0.06;
        tau = 0.29;
    elseif deltaU(2)>=36 && deltaU(2)<=100
        kFlujo = -0.035;
        kTemperatura = -0.046;
        tau = 0.29;
    end

elseif deltaU(1)>=41 && deltaU(1)<=50
    if deltaU(2)>=0 && deltaU(2)<=35
        kFlujo = -0.06;
        kTemperatura = -0.049;
        tau = 0.1;
    elseif deltaU(2)>=36 && deltaU(2)<=100
        kFlujo = -0.053;
        kTemperatura = -0.05;
        tau = 0.1;
    end

elseif deltaU(1)>=51 && deltaU(1)<=60
    if deltaU(2)>=0 && deltaU(2)<=35
        kFlujo = -0.05;
        kTemperatura = -0.04;
        tau = 0.1;
    elseif deltaU(2)>=36 && deltaU(2)<=100
        kFlujo = -0.03;
        kTemperatura = -0.04;
        tau = 0.1;
    end

elseif deltaU(1)>=61 && deltaU(1)<=70
    if deltaU(2)>=0 && deltaU(2)<=35
        kFlujo = -0.05;

```

```

        kTemperatura = -0.05;
        tau = 0.1;
    elseif deltaU(2)>=36 && deltaU(2)<=100
        kFlujo = -0.03;
        kTemperatura = -0.04;
        tau = 0.08;
    end

elseif deltaU(1)>=71 && deltaU(1)<=80
    if deltaU(2)>=0 && deltaU(2)<=35
        kFlujo = -0.04;
        kTemperatura = -0.04;
        tau = 0.06;
    elseif deltaU(2)>=36 && deltaU(2)<=100
        kFlujo = -0.041;
        kTemperatura = -0.026;
        tau = 0.05;
    end

elseif deltaU(1)>=81 && deltaU(1)<=130
    if deltaU(2)>=0 && deltaU(2)<=100
        kFlujo = -0.041;
        kTemperatura = -0.033;
        tau = 0.05;
    end

end
GF(loopCount) = kFlujo;
GT(loopCount) = kTemperatura;
Ttau(loopCount) = tau;

yOutput = ((kFlujo*deltaU(1))+(kTemperatura*deltaU(2)))*(1-exp(-t/tau))
+ initialHumidity;
du = [deltaU(1);deltaU(2)];

yModelo = Sb1*deltaU + yPredictedTrajectory;

Wp(loopCount) = yOutput;

Time(loopCount) = t;

CurrentHumidity(loopCount) = initialHumidity;

if Wp(loopCount)<setPoint
    break
end

error = Wp(loopCount) - yModelo(loopCount);
yPredictedTrajectory = M*yPredictedTrajectory + Sx*du +
error*ones(n(1,1),1);

```



```

    loopCount = loopCount + 1;
    counter=counter+2;
end
loopCount = loopCount - 1;
    subplot(2,1,1); plot(Time(1:loopCount),Wp(1:loopCount),'-
* ',Time(1:loopCount),yModelo(1:loopCount),'--
',Time(1:loopCount),yReferenceTrajectory(1:loopCount),'g');
    subplot(2,1,2); plot(Time(1:loopCount),CurrentQ(1:loopCount),'-
* ',Time(1:loopCount),CurrentT(1:loopCount));

```

### C. Model Predictive Control Toolbox®

The screenshot displays the 'Control and Estimation Tools Manager' window. On the left is a 'Workspace' pane with a tree view containing 'MPCdesign', 'Plant models', 'Controllers', and 'Scenarios'. The main area is titled 'MPC structure overview' and contains a block diagram. The diagram shows an 'MPC' block receiving 'Setpoints (reference)' and '0 Measured disturbances'. It outputs '2 Manipulated variables' to an 'Inputs' block, which then feeds into a 'Plant' block. The 'Plant' block also receives '0 Unmeasured disturbances' and outputs '1 Measured' and '0 Unmeasured' signals to an 'Outputs' block. Below the diagram are three buttons: 'Import Plant ...', 'Import Controller ...', and 'Help'.

Below the diagram are two tables for signal properties:

**Input signal properties**

Name	Type	Description	Units	Nominal
Airflow	Manipulated		m <sup>3</sup> /hr	0.0
Temperature	Manipulated		°C	0.0

**Output signal properties**

Name	Type	Description	Units	Nominal
Moisture Content	Measured			0.0